2018•2019

Faculteit Industriële ingenieurswetenschappen

master in de industriële wetenschappen: biochemie

Masterthesis

Modulation of adenovirus replication by antiviral and immunosuppressive agents

PROMOTOR :

dr. ir. Kristel SNIEGOWSKI

PROMOTOR :

Prof. dr. Lieve NAESENS

COPROMOTOR :

ir. Leentje PERSOONS

Simona Cecchi

Scriptie ingediend tot het behalen van de graad van master in de industriële wetenschappen: biochemie

Gezamenlijke opleiding UHasselt en KU Leuven

2018•2019

Faculteit Industriële ingenieurswetenschappen

master in de industriële wetenschappen: biochemie

Masterthesis

Modulation of adenovirus replication by antiviral and immunosuppressive agents

PROMOTOR :

dr. ir. Kristel SNIEGOWSKI

PROMOTOR :

Prof. dr. Lieve NAESENS

COPROMOTOR :

ir. Leentje PERSOONS

Simona Cecchi

Scriptie ingediend tot het behalen van de graad van master in de industriële wetenschappen: biochemie

UHASSELT

KU LEUVEN

A word of appreciation

Making a difference in this world by contributing to a project which can help thousands of people's lives and my interest for continuous development in the healthcare sector are the reasons of interest for this master thesis. It is my passion to not only find out, but to do research for future generations.

In truth, I could not have achieved my master thesis without a strong support group. First of all, my parents, who supported me with love and understanding during my studies. I would also like to extend my deepest gratitude to my supervisor Lieve Naesens and co-supervisor Leentje Persoons together with Bianca and their research group, each of whom has provided patient advice and guidance throughout my internship. Furthermore, I would like to thank Geert and Evelien for the introduction of various techniques used for my experiments. Thank you all for your unwavering support.

Table of contents

List of tables

List of figures

Abbreviations

4EBP1	4E-binding protein 1
5-Fu	5-fluorouracil
AdV	adenovirus
AdV Pol	AdV polymerase
AKT or PKB	Protein kinase B
Ara-A	vidarabine
Ara-C	cytarabine
bp	base pairs
CAR	coxsackie and adenovirus receptor
CC_{50}	50% cytotoxic concentration
$CCID_{50}$	culture-infective dose 50%
CDV	cidofovir
CNI's	calcineurin inhibitors
CPE	cytopathic effect
CTL	cytolytic T-cell
DBP	DNA-binding protein
ddC	zalcitabine
DMEM 1x	Dulbecco's Modified Eagle Medium 1x
ds	double-stranded
DS-10,000	dextran sulfate
DSG2	desmoglein-2
E	early region
EC_{50}	50% effective concentration
EDTA	ethylenediamine tetraacetic acid
eIF4E	eukaryotic translation initiation factor 4E
EKC	epidemic keratoconjunctivitis
ELISA	enzyme-linked immunosorbent assay
ERK	extracellular signal regulated kinase
FACS	fluorescence-activated cell sorting
FDA	Food and Drug Administration
FddT	alovudine
FKBP12	FK-binding protein 12
FW	forward
GFP	green fluorescent protein
GNA	*Galanthus nivalis* agglutinin
GVHD	graft-versus-host disease
GVL	graft-versus-leukaemia
HEK	human embryonic kidney
HEL	human embryonic lung
HHA	*Hippeastrum hybrid* agglutinin
HI-FCS	heat-inactivated fetal calf serum
HRP	horseradish peroxidase
HSCT	hematopoietic stem cell transplantation

i.v.	intravenous
ICTV	International Committee on Taxonomy of Viruses
Ig	immunoglobulin
IL-2	interleukin-2
INSR	insulin receptor
ITR	inverted terminal repetitions
kb	kilo base pairs
KCs	Kupffer cells
kDa	kilodalton
L	late region
LFL	leflunomide
LSECs	liver sinusoidal endothelial cells
MCC	minimal cytotoxic concentration
MCP or CD46	membrane cofactor protein
MLP	major late promotor
MMF	mycophenolate mofetil
MPA	mycophenolic acid
MPS	mycophenolate sodium
MTOC	microtubule-organizing center
mTOR	mammalian target of rapamycin
NESs	nuclear export signals
NFAT	nuclear factor of activated T-cells
NLSs	nuclear localization signals
OD	optical density
ORI	origins of replication
p.i.	post infection
PBS	phosphate-buffered saline
PCR	polymerase chain reaction
PE	phycoerythrin
PI3K	phosphatidylinositol-3-OH kinase
PKC	protein kinase C
PMEG	9-(2-Phosphonylmethoxyethyl) guanine
PRM-S	pradimicine-S
pTP	precursor of the TP
Ras	small GTPase protein
RBV	ribavirin
RGD	Arginine-Glycine-Aspartatic acid
RKT	receptor tyrosine kinase
RV	reverse
SN	supernatants
TFT	trifluorothymidine
TP	terminal protein
UDA	*Urtica dioica* agglutinin
WGA	wheat germ agglutinin lectin

Abstract

Human adenoviruses (AdVs) are widespread pathogens transmitted by aerogenic or direct contact. In otherwise healthy persons, AdVs infections mostly cause self-limiting respiratory disease, diarrhea and ocular infections. At the same time, AdVs can be life-threatening for immunocompromised individuals. Children in particular are vulnerable when receiving immunosuppressive or cytostatic drugs in the context of hematopoietic stem cell transplantation. Despite the clear medical need, there is no approved anti-AdV therapy.

The aim of this master thesis is to investigate whether and how antiviral, immunosuppressive or cytostatic drugs mediate the AdV life cycle. A series of these drugs were tested in AdV-infected human embryonic lung (HEL) cells and A549 cancer cells, to assess their antiviral (or proviral) effect on AdV replication. To this goal, suitable procedures were developed. Virus replication was monitored by (fluorescence) microscopy, cell viability assay and qPCR for viral DNA.

Anti-AdV activity was observed for the immunosuppressants sirolimus and methotrexate, and reference antiviral agent cidofovir. Sirolimus was only active in HEL cells. An attempt was made to implement an ELISA assay for mTOR pathway activity, the target of sirolimus. More research is needed to understand the different impact of sirolimus on AdV infection in the two cell lines.

The results indicate that some immunosuppressants can modulate AdV replication. Besides, the methods developed are relevant for ongoing anti-AdV drug discovery projects.

Abstract

Humane adenovirussen (AdVs) zijn wijdverspreide pathogenen die worden overgedragen door aerogeen of direct contact. Bij overigens gezonde personen veroorzaken AdVs meestal zelfgenezende respiratoire ziekten, diarree en ooginfecties. Ook veroorzaken AdVs regelmatig ernstige tot levensbedreigende ziekten bij immuungecompromitteerde individuen. Een bijzonder kwetsbare populatie zijn kinderen die immunosuppressieve of cytostatische geneesmiddelen krijgen in de context van hematopoietische stamcel-trasplantatie. Ondanks de duidelijke medische noodzaak is er geen goedgekeurde anti-AdV-therapie.

Het doel van deze masterproef is om te onderzoeken of en hoe antivirale, immunosuppressieve of cytostatische geneesmiddelen de AdV-levenscyclus in verschillende celtypen mediëren. Een reeks van deze geneesmiddelen werd getest in AdV geïnfecteerde menselijke embryonale long (HEL) cellen en A549-kankercellen om hun antivirale (of provirale) effecten op AdV-replicatie te bepalen. Hiertoe zijn geschikte procedures ontwikkeld. Virusreplicatie werd gevolgd door (fluorescentie) microscopie, cel levensvatbaarheidsassay en qPCR voor viraal DNA.

Er werd anti-AdV-activiteit waargenomen voor de immunosuppressiva sirolimus en methotrexaat en het referentie antiviraal middel cidofovir. Sirolimus was actief in HEL-cellen, maar niet in A549-kankercellen. Er is een poging gedaan om een ELISA-test te implementeren voor mTOR-route-activiteit, het doelwit van sirolimus. Meer onderzoek is nodig om de verschillende effecten van sirolimus op AdV-infectie in de twee cellijnen te begrijpen.

De resultaten geven aan dat sommige immunosuppressiva AdV-replicatie kunnen moduleren. Bovendien zijn de ontwikkelde methoden relevant voor de ontdekking van anti-AdV-geneesmiddelen.

1. Introduction

This thesis project was carried out under the guidance of Prof. Dr. Lieve Naesens, at the Laboratory of Virology and Chemotherapy of the Rega Institute, located at the 'Gasthuisberg' campus of KU Leuven. This campus is unique as it combines within a very compact area a large university hospital and cutting-edge facilities for biomedical research such as the Rega Institute. This close contact enables easy access to clinical samples and multidisciplinary or translational projects.

Within the multidisciplinary Rega institute, the Laboratory of Virology and Chemotherapy has an important core infrastructure with a wide variety of biological, biophysical and biochemical equipment. It is equipped with instrumentation for cell culture and virus experiments (including creation of mutant viruses); animal experimentation; deep-sequencing; high-content fluorescence imaging; confocal microscopy; multi-parameter flow cytometry; chemiluminescence detection; protein, DNA and RNA analysis; protein expression and purification; surface-plasmon resonance; biochemical studies requiring radiolabeled precursors; high-performance liquid chromatography and X-ray crystallography.

The central research aim of Prof. L. Naesens is to develop new antiviral concepts with high relevance for human medicine. The research group investigates respiratory viruses, namely influenza, corona- and adenoviruses. All topics have an innovative character, relevance for pharmaceutical drug development and a potentially high impact on human health.

This thesis project focuses on human adenoviruses (AdVs), a class of widespread viral pathogens with diverse clinical manifestations. AdV is transmitted via the air through aerosols generated by sneezing or coughing, or through the fecal-oral route. The naked virus particles are very stable outside the host, on surfaces and in water, hence infection can occur by direct contact. Most AdV infections occur in early childhood and are commonly associated with self-limited, febrile upper respiratory tract illnesses. Severe and sometimes fatal infections can occur in immunocompromised hosts, neonates, and, rarely, healthy children and adults. Furthermore, different serotypes of AdVs can infect various organs such as the respiratory, gastrointestinal and lower urinary tract. In addition, AdV infections can occur in the eyes, causing epidemic keratoconjunctivitis (EKC). Other rare manifestations are cardiac, genitourinary, and neurologic diseases. In short, AdVs target a broad group of individuals with diverse clinical syndromes [1-3].

Despite the clear medical need, no approved antiviral therapy exists to treat fulminant systemic AdV infections. This project is intended to fill this gap by a rational and dual approach, investigating on one hand how host-targeting drugs used in the risk population may affect AdV replication, and on the other hand how immunosuppressive agents can modulate the first stage of virus replication. This project is built on previous expertise of L. Naesens in this domain. This knowledge base will now be expanded with methods for in-depth mechanistic investigations [1].

It is anticipated that some immunosuppressant or cytostatic agents may act as antivirals by inhibiting AdV replication. This is indeed supported by a pilot study conducted by L. Persoons, showing that several anti-cancer drugs (e.g. cladribine, gemcitabine and methotrexate) exert clear anti-AdV activity in cell culture. This creates opportunities for designing entirely novel classes of anti-AdV therapeutics, which are highly needed in the clinic.

Vice versa, a reported analysis of clinical data indicated that the risk for severe AdV infections depends on the immunosuppressive or myeloablative regimen, with some drugs (such as fludarabine) showing a particularly strong association [2].

The main objectives of this master thesis are:
(1) to investigate whether and how immunosuppressive or cytostatic drugs mediate the AdV life cycle in different cell types;
(2) to optimize suitable procedures to conduct these studies.

To achieve these objectives, a detailed study was performed of the direct impact of these drugs on the course of AdV replication. The cell culture data will reveal which 'proviral' drugs increase the level of AdV replication and provide guidance for selecting the best immunosuppressive drug regimens for hematopoietic stem cell transplantation (HSCT) patients.

A broad panel of immunosuppressive and cytostatic agents were tested against five AdV types to cover the different AdV subgroups. Virus replication will be monitored by microscopic methods and polymerase chain reaction (PCR). Next, an enzyme-linked immunosorbent assay (ELISA) method will be used to investigate the biochemical basis for the observed pro- or antiviral effects.

Since this study involved different AdV types and cell lines, insight in the precise virus entry route was required. Therefore, fluorescence-activated cell sorting (FACS) analysis was established for quantification of the two major AdV receptors, i.e. membrane cofactor protein (MCP or CD46) and coxsackie and adenovirus receptor (CAR).

2. Literature study

2.1 Clinical manifestations of human adenoviruses

In **immunocompetent persons**, AdV infections are mostly self-limited and occasionally asymptomatic. Symptomatic infections are associated with only some of the known AdV serotypes. AdV infections of the respiratory tract account for 5 to 10 % of all respiratory infections in children. Besides, AdV infections of the gastrointestinal tract are responsible for 5 to 15 % of acute diarrheal illness in children. Some AdV types can infect the urinary tract and cause hemorrhagic cystitis, which mostly occurs in boys. Myocarditis, hepatitis and meningoencephalitis are rare manifestations of AdV infection [1, 3, 4].

In contrast, in **immunocompromised individuals**, AdVs frequently cause aggressive and life-threatening infections. Some examples are infants and young children whose immune system is still immature; individuals suffering from primary immunodeficiency or HIV infection; cancer patients receiving chemotherapy; and hematopoietic stem cell transplantation (HSCT) and solid organ transplant recipients. Given the growing practice of transplantation accompanied by strong immunosuppressive therapy, the incidence of severe AdV infections has gradually increased. A delicate balance exists between applying adequate immunosuppressive treatment to prevent allograft rejection or graft-versus-host disease (GVHD), while at the same time limiting the risk of AdV (or other opportunistic) infections [1, 5].

One particular risk group are young children with leukemia undergoing HSCT. These pediatric patients are particularly prone to disseminated AdV infections with high morbidity and mortality, and account for the largest number of severe AdV infections. Until now, no study has been conducted to examine how AdV replication is affected by the diverse immunosuppressive or cytostatic drugs given to HSCT or cancer patients [1, 6].

The **ocular manifestations** of AdVs, known as epidemic keratoconjunctivitis (EKC), represent a distinct medical problem. This highly contagious disease, encountered year-round, can occur at any age and independent of the person's immune status. In 70% of the cases, patients seek medical care because of intolerable symptoms. Common clinical signs are redness, inflammation, eye lid swelling, impaired vision, and pain lasting for two to three weeks. Despite the clear medical need, no approved antiviral therapy exists to treat AdV EKC [7].

2.2 Taxonomy and classification

The International Committee on Taxonomy of Viruses (ICTV) has classified human AdVs under the *Adenoviridae* family that is divided into five genera: *Atadenovirus* (infecting a broad range of hosts); *Aviadenovirus* (infecting birds); *Ichtadenovirus* (infecting fish); *Siadenovirus* (infecting frogs and some birds); and *Mastadenovirus* (infecting mammals). Human AdVs belong to the *Mastadenovirus* genus and are grouped in seven species ("subgroups") referred to as AdV-A to AdV-G. Further classification of the different AdV types, formerly called "serotypes", is, among other characteristics, based on serology, hemagglutinating properties and oncogenicity in rodents.

There is a correlation between AdV species and tissue tropism (see Table 1). The latter is dependent on AdV receptor usage, more specifically the initial high affinity binding recognition between the AdV fiber knob and a specific cell surface receptor. At the moment, 90 different human AdV types are known with most types belonging to species AdV-D followed by species AdV-B. Gene recombination for capsid components (hexon, penton and fiber) is the main factor contributing to inter-species diversity. In contrast, continuous selection of capsid gene sequences is the main basis for intra-species diversity [4, 8, 9].

Table 1. Classification and tissue tropism of human AdV types.

Species	AdV types	Organ tropism
A	12,18,31,61	Enteric and respiratory
B	3, 7, 11, 14,16, 21, 34, 35, 50, 55, 66, 68, 76-79	Renal, respiratory and ocular
C	1, 2, 5, 6, 57,89	Respiratory, ocular, hepatic and lymphoid
D	8-10, 13, 15, 17, 19, 20, 22-30, 32, 33, 36-39, 42-49, 51, 53, 54, 56, 58-60, 62-65, 67, 69-75, 80-88, 90	Ocular and enteric
E	4	Respiratory and ocular
F	40, 41	Enteric
G	52	Enteric

2.3 Virion structure

As shown in Fig. 1, the AdV virion consists of a non-enveloped capsid with a characteristic icosahedral morphology. Mature virions are around 70 to 100 nm in diameter and consist of a DNA-protein core complex encased in a capsid shell that is composed of three capsid proteins. The hexon is the most abundant one and provides the triangular facets of the capsid. The penton protein is located at each of the twelve vertices, whereas the thin trimeric fiber protein protrudes from the capsid with its distal globular knob ready for initial cell attachment. Both the penton and fiber are involved in the binding interaction between the viral capsid and surface of the host cell.

The minor proteins IIIa, VI, VIII and IX are capsid-associated proteins with a role in virion assembly, stability and disassembly during infection.

Inside the capsid, various core proteins are present and a linear double-stranded (ds) DNA genome of about 36,000 bp with a covalently attached terminal protein (TP) at each 5’ end. The linear genome is condensed by three basic proteins, V, VII and Mu. These DNA-binding proteins are responsible for condensation of the DNA into a nucleosome-like structure, and connection of the DNA to the capsid. Also, core protein IVa2 was suggested to be a transcriptional activator and involved in DNA packaging in the virion core. The last known protein inside the core is the AdV protease, which is essential to render the virion infective [1, 4].

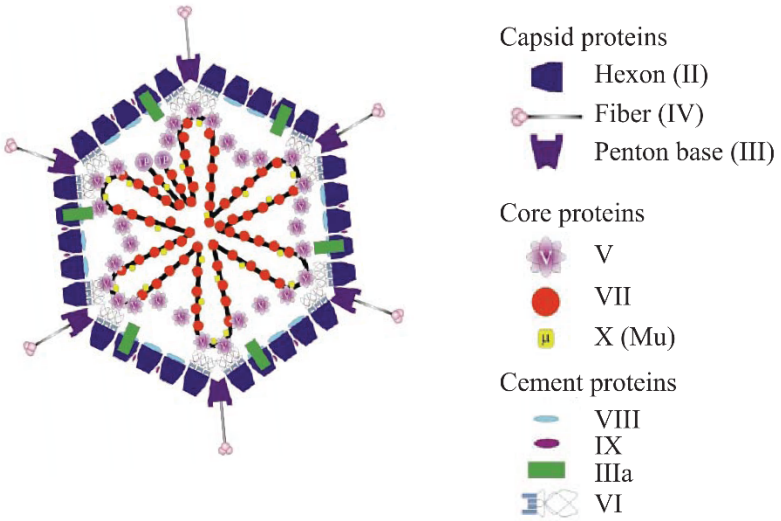

Figure 1. Structure and composition of AdV virions. Source: Lenaerts *et al.* [3].

2.4 Virus life cycle

The life cycle of AdVs can be divided into three stages: (i) cell surface binding followed by internalization and nuclear transport; (ii) replication; and (iii) assembly and release. The cycle is summarized in Fig. 2 and detailed in more detail in the text below.

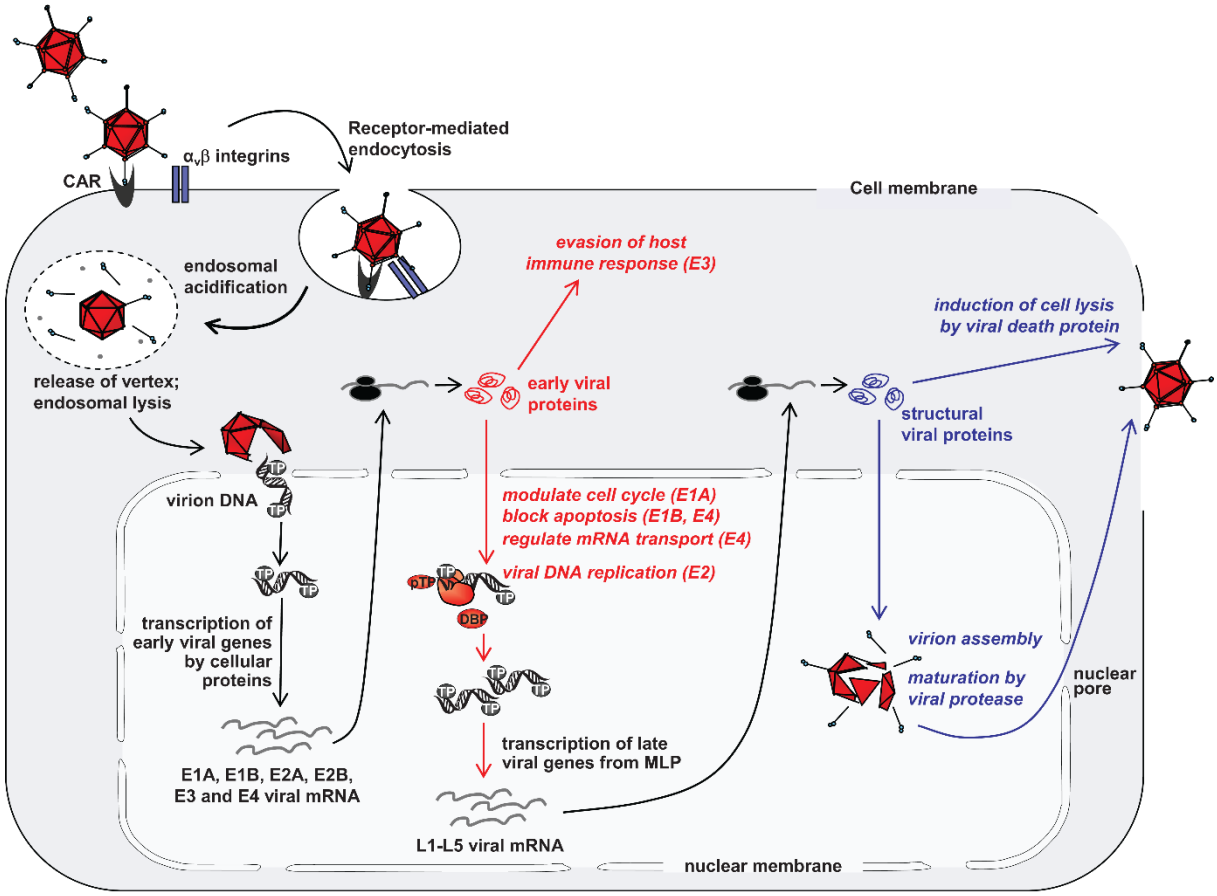

Figure 2. The adenovirus life cycle. CAR, coxsackie-adenovirus receptor; DBP, DNA-binding protein; E, early; L, late; MLP, major late promoter; pTP, precursor terminal protein; TP, terminal protein. Note that not all AdV types use CAR as the primary binding receptor. Source: Lenaerts *et al.* [3].

2.4.1 Adenovirus binding to host cells

The virus life cycle starts with recognition of the target cell, which is mediated by the globular knob domain of the fiber. This initial contact is a major determinant in AdV type-specific tissue tropism, since different types have different fibers recognizing specific cell surface receptors. The first identified AdV receptor, called coxsackie and adenovirus receptor (CAR), is abundantly expressed in a wide variety of tissues. As explained in detail in Section 2.5 at page 23, some AdV species do not recognize CAR and instead use other cell surface receptors [4, 10].

2.4.2 Virus entry and transport to nucleus

Internalization of the virus particle is mediated by association of the AdV penton base with cell surface integrins, functioning as co-receptors. The penton contains an integrin recognition motif consisting of three amino acids [arginine-glycine-aspartic acid (RGD)]. This penton base-integrin interaction triggers phosphatidylinositol-3-OH kinase (PI3K), an intracellular lipid kinase that acts like a secondary messenger, resulting in actin reorganization and endocytosis of the virion by clathrin-coated vesicles. Clathrin-mediated endocytosis is the best known AdV entry pathway, although species B and C appear to also enter via macropinocytosis [4, 10].

During endocytosis, the virus starts to dismantle itself. The fiber proteins start to detach from the penton base at the plasma membrane, followed by a conformational change that exposes hydrophobic parts and weakens the capsid. After release of different internal proteins, the processes of virion uncoating and endosomal escape proceed at high speed. After initial cell binding, it takes approximately 15 min to detect free virions in the cytoplasm. Although the endosomal escape mechanism is not precisely understood, it is clearly related to acidification, endosomal lysis and escape of the virions into the cytoplasm, followed by their translocation along microtubules towards the nucleopore complex. This active transport is mediated by a motor protein called dynein, which scrolls over the microtubules towards the microtubule-organizing center (MTOC) near the nucleus [3, 4].
Once the capsid arrives at the MTOC, near the nucleus, it needs to dock the nuclear pore to get through. Therefore, interaction of the capsid and nuclear pore proteins CAN/Nup214 is needed to facilitate docking. This interaction also allows nuclear histone H1 proteins to dock to hexon proteins whereby importation of β proteins can occur that cause diffusion of viral DNA into the nucleus. Once in the nucleus, DNA replication can start [1, 3, 4, 10].

2.4.3 Organization and replication of the AdV genome

Within 40 hours, an infected cell produces approximately one million copies of viral DNA. The 36 kbp genome can produce over 40 proteins. What makes this possible is the effective organization of the genome [4]. According to the time in which these genes are expressed, the genome is divided into an early (E) and late (L) region. There are eight polymerase II transcription units located at each strand of the genome: five early units (E1A, E1B, E2, E3, E4), two intermediate (IX and IVa2) and one late (L1-L5) [3, 4].

In addition, two delayed-early transcription units are expressed, i.e. proteins IX and IVa2. Besides its role as capsid cement, the IX protein also functions in transcription activation. The

IVa2 protein triggers expression of the late units by activating the major late promotor (MLP) when progeny AdV genomes accumulate in the nucleus. During the late phase of infection, production of viral mRNA and proteins is accompanied by host cell shut-off. The mature late transcripts encode the viral structural proteins and proteins that are required for encapsidation and maturation of virus particles. One day after infection, virions start to assemble, which is mediated by interactions of IVa2, L1 and L4 proteins and the packaging sequence at one end of the genome. Two days later, AdV progeny is released by cell lysis which is triggered by the virus-encoded death protein [3].

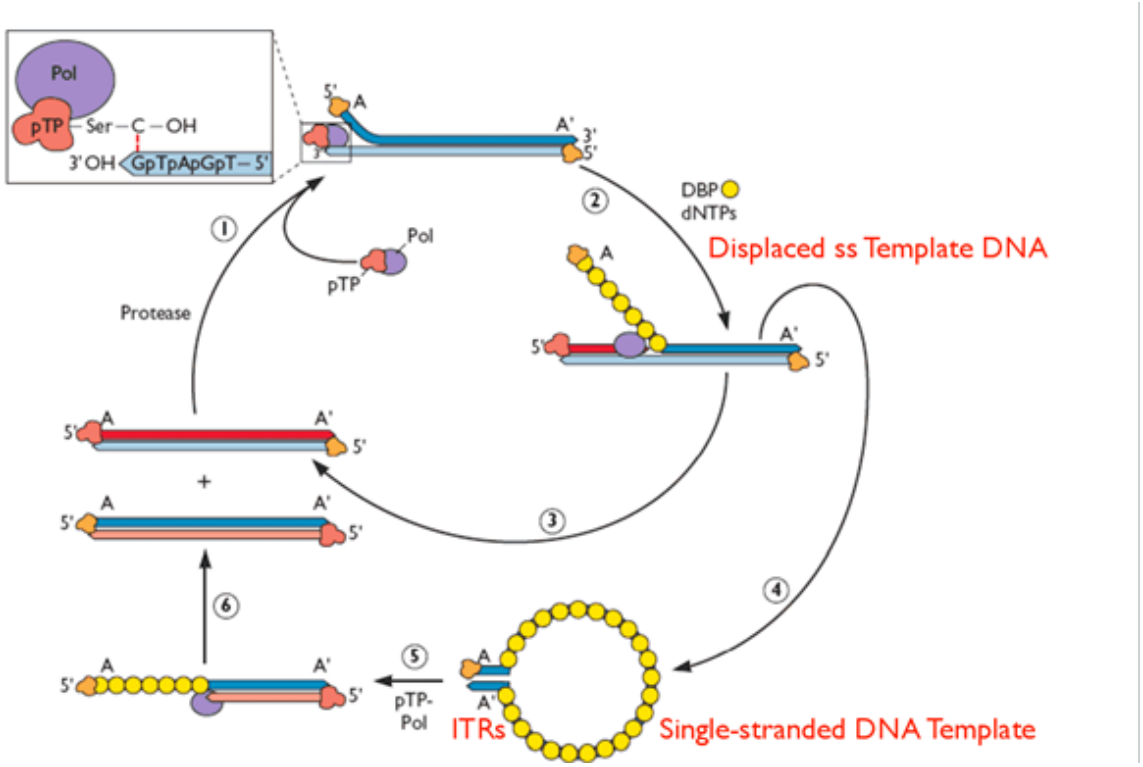

Figure 3. Replication of adenoviral DNA. Source: Dewi *et al.* [11].

AdV replication requires three viral proteins encoded by E2 genes: precursor of the terminal protein (pTP), AdV polymerase (AdV Pol), and the DNA-binding protein (DBP).

The first step in Fig. 3 shows the assembly of the viral pTP and AdV Pol into a preinitiation complex at each terminal origin of replication (ORI) which activates covalent linkage of dCMP to a specific serine residue in pTP by the DNA Pol. The free 3'-OH group of pTP-dCMP primers continuous synthesis in the 5' to 3' direction by AdV pol (step2). This reaction also requires the viral E2 single-stranded-DBP, which coats the displaced second strand of the template DNA molecule, and a cellular topoisomerase. At both end of the linear ds genome there are inverted terminal repetitions (ITR) of about 100 bp. Within the ITR, two identical origins of replication (ORI) are present and both parental strands can be replicated by this displacement mechanism (step 3). Reannealing of the complementary ITR initially forms a short duplex stem identical to the terminus of the ds genome (step 4). The origin re-formed in this way directs a new cycle of protein priming and continuous DNA synthesis (step 5 and 6). The pTP is cleaved by the viral protease to the terminal protein (TP) during maturation of viral particles [8, 12].

2.4.4 Assembly and release

The last step is assembly, which takes place in the nucleus, and release of virions. Both import and export trafficking over the nuclear pore complex are required, therefore AdV proteins utilize the cellular pathways for nuclear transportation by presenting nuclear localization signals (NLSs) and nuclear export signals (NESs). After DNA replication, the viral DNA is injected into the empty capsids, although other theories suggest that the capsid is formed around the DNA core. Also, incomplete virions (containing only capsid) are thought to induce inflammation without any gene expression. On the other hand, complete virions require maturation mediated by the AdV protease to become infective progeny virions [4].

2.5 Zoom on receptor use

Here the receptor usage of different AdV types will be described in more detail, since this is relevant to understand the diverse AdV tissue tropism and disease manifestations, and to design potential AdV entry inhibitors for antiviral drug development.
This topic is also important for AdV vector usage. AdV vectors, in particular AdV-5, are the most popular vectors to potentially treat many diverse types of cancer. AdV-based vectors are also considered to treat cardiovascular diseases such as ischemia, artery diseases and angina. Finally, AdVs are being developed as vaccine vectors to treat or prevent infections like HIV or Ebola. The popularity of AdV-5 as a gene vector is related to its wide tissue tropism, yet a main problem is its accumulation in and clearance by the liver. Therefore, there is much interest in using other AdV types, provided that their cell entry mechanisms are well understood, since this determines the targeted tissue for gene transfer.

Fig. 4 provides an overview of currently known AdV cell surface receptors. The diverse receptor use is related to differences in fiber amino acid sequence; the length and flexibility of the fiber shaft; and net charge of the fiber knob [3, 13].

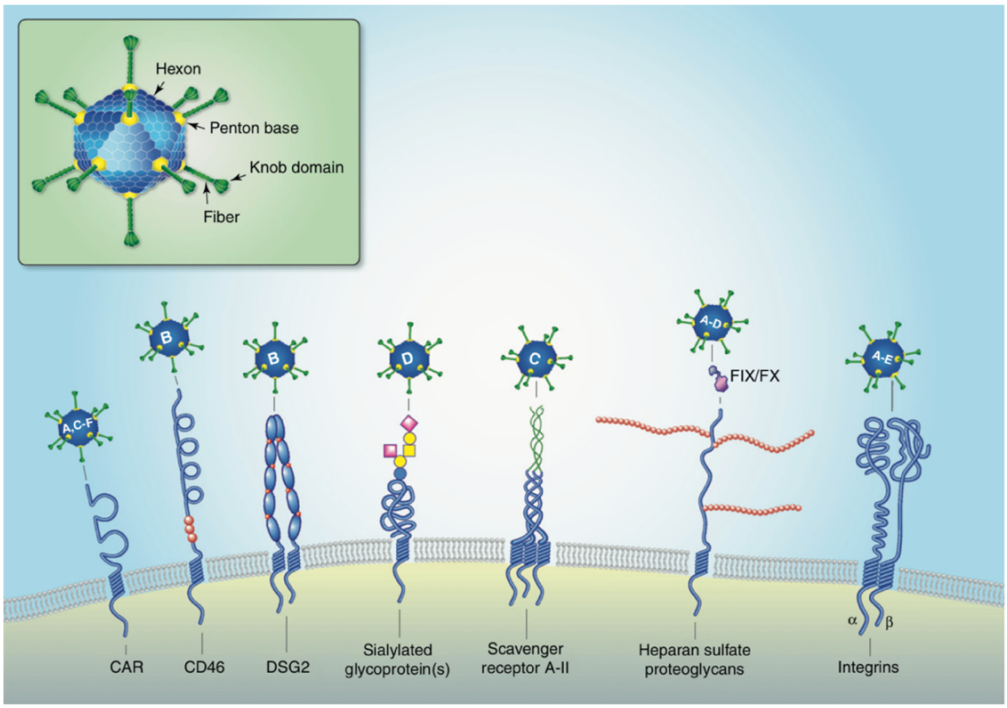

Figure 4. Overview of the best characterized receptors used by human AdVs. Note that AdV species G is not shown because the receptors for these AdV types remain to be determined. Source: N. Arnberg *et al.* [13].

2.5.1 The coxsackie and adenovirus receptor

The first known AdV receptor, CAR, is abundantly expressed in a wide variety of tissues and, at least in vitro, functions as a high affinity receptor for the fiber protein of most AdV species A and C–F viruses, but not for species B. It belongs to the immunoglobulin superfamily and forms intercellular homodimers at epithelial cell-cell junctions. The in vivo role of CAR is not fully clear since most epithelial cells express CAR at their basolateral membrane, whereas AdVs are thought to bind and initiate infection at the apical side of the cells. Some investigations have indicated that the CAR-fiber interaction may mainly function to facilitate escape of virions from the site of infection. This is due to an excess of fiber and pentons that are produced during infection that bind to CAR and thereby disrupt the cellular tight-junctions allowing the virus escape [13, 14].

2.5.2 Integrins

Integrins are heterodimeric proteins consisting of an α and β subunit which contribute to cell-cell adhesion alike CAR. Integrins transfer signals into the cell and promoting AdV entry in vivo. The interaction is mediated by the integrin-recognition RGD motif that is present in the AdV penton base of all AdVs except species F. Most integrins are localized at the basolateral side of the cell, however they can be relocalized to the apical side or upregulated on cells due to various stimuli [4, 13].

2.5.3 The membrane cofactor protein of CD46 receptor

The membrane cofactor protein (MCP or CD46) belongs to the regulators of complement activation. The complement pathway is part of the immune system. It enhances (complements) the ability of antibodies and phagocytic cells to clear microbes and infected or damaged cells; promotes inflammation; and attacks the pathogen's cell membrane. The main function of CD46 is to protect healthy cells from complement-mediated degradation. This receptor is only used by AdV species B and AdV-37 (species D). Some species B AdVs prefer to interact with the structurally related CD80/CD86 co-stimulatory molecules on antigen presenting cells, or another unidentified glycoprotein expressed on human stem and tumor cells [3, 13, 15].

2.5.4 Desmoglein-2

Desmoglein-2 (DSG2) is a cell adhesion molecule similar to CAR, however it belongs to the cadherin superfamily. Among the known species B AdVs, there are some (namely AdV-3, -7, -11 and -14) that use DSG2 as an additional or exclusive cellular receptor, opposite to AdV-16, -21, -35 and -50 which use CD46 only. The virion interaction with DSG2 appears to be more complex compared to that with CD46, since it involves binding of both the fiber and penton base [13].

2.5.5 Sialic acid-containing glycoproteins

Sialic acid-containing glycoproteins were identified as cell receptors for species D AdVs such as AdV-8, -19a and -37 which are common causes of EKC. The fiber knob of these AdVs can interact with sialic acid-containing glycan motifs of some cell surface glycoproteins (Fig. 4). Similar motifs are present in the GD1a ganglioside which by itself is not an AdV receptor. The glycans serving as receptors appear to be attached to membrane proteins on corneal and conjunctival cells. The sialic-binding fiber amino acids are conserved in several species D AdVs [3, 13].

2.5.6 Scavenger receptor A-II and heparan sulfate proteoglycans

Some AdV types of species A to D can bind Kupffer cells (KCs), hepatocytes and liver sinusoidal endothelial cells (LSECs). KCs are targeted through interactions with scavenger receptors that bind directly to hypervariable regions of the AdV hexon, but also indirectly via IgM and complement components. The mechanisms to enter LSECs are less well characterized but it has been suggested that the RGD motif in the viral penton base and specific cellular integrins are involved. As for AdV binding to hepatocytes, this has been studied in much detail and involves coagulation factors that bind to heparan sulfate-containing membrane glycoproteins on the cell surface and to hypervariable regions in the AdV hexon protein [13].

2.6 Advanced strategies to suppress severe HAdV infections

In the first part there was a detailed description about Advs and their clinical manifestations, structures, life cycle and receptor use. In this second part there will be looked at how they can be suppressed. The drugs and therapies described herein have already been preceded by research.

2.6.1 Antiviral drugs for systemic AdV infections

The need for an effective antiviral therapy against AdVs is increasing, due to the growing incidence of severe AdV infections in immunocompromised individuals. Two commercially available antiviral drugs, cidofovir and ribavirin, have been used off-license in clinical studies. The broad DNA virus inhibitor cidofovir [CDV; (S)-HPMPC; (S)-1-(3-hydroxy-2-phosphonylmethoxypropyl)cytosine)] belongs to the acyclic nucleoside phosphonates, an antiviral drug class discovered at the Rega Institute. After entering the cell by endocytosis, CDV is converted into an active metabolite through two consecutive phosphorylation steps by cellular enzymes. The diphosphate form (CDV-pp) then acts as a structural analogue of dCTP, and is recognized by AdV Pol as an alternative substrate. Following incorporation of CDV into the nascent AdV DNA strand, non-obligate chain termination occurs leading to interruption of viral DNA synthesis [16]. Ribavirin (1-β-D-ribofuranosyl-1,3,4-triazole-3-carboxamide), is a purine nucleoside analogue with broad antiviral activity against several viruses which also requires phosphorylation by cellular enzymes. The monophosphate metabolite of ribavirin inhibits the cellular IMP dehydrogenase enzyme, which results in depletion of the cellular GTP pool. This explains the broad anti-RNA virus effect of ribavirin, whereas for DNA viruses like AdVs, the antiviral mechanism is not evident.
Cidofovir and ribavirin have been used in AdV-infected immunocompromised individuals and both successes and failures have been reported. Both drugs have significant side-effects (in particular, nephrotoxicity for cidofovir and anemia for ribavirin). The “European guidelines for treatment of AdV infections 2011” by Matthes-Martin *et al*. state that ribavirin is not recommended for treatment of AdV infections [3, 4, 17, 18].

The newer antiviral drug brincidofovir is an orally bioavailable lipid conjugate of cidofovir. Compared to unmodified cidofovir, brincidofovir has superior anti-DNA virus potency in vitro and in vivo. Since brincidofovir was found to be free of nephrotoxicity, it proceeded to Phase 3 clinical studies as an attractive candidate for anti-DNA virus prophylaxis in immunocompromised individuals. Unfortunately, oral use of this drug proved associated with severe gastrointestinal toxicity, and hence current studies are looking at an intravenous (i.v.) formulation of brincidofovir. In any case, the sustained virologic response in patients who had failed CDV treatment suggest that brincidofovir may be an effective treatment for severe AdV disease. Although encouraging, these safety data must be interpreted with caution [18, 19].

2.6.2 Adoptive T-cell transfer therapy

The immunotherapeutic approach consisting of adoptive AdV-specific T-cell transfer could be an alternative for antiviral chemotherapy in immunocompromised individuals. It involves infusion of AdV-specific T-cells that can be selected directly from peripheral blood or selectively expanded in vitro. Zandvliet *et al.* demonstrated that AdV hexon-specific T-cell adoptive immunotherapy generated CD8+ and CD4+ T-cell responses that cleared AdV infection in immunocompromised individuals. These infusions were devoid of toxicity, and some patients showed a significant decrease in AdV DNA in peripheral blood and stool. It was suggested that the T-cell effect was independent of the infused cell dose and that even low numbers of transferred AdV-specific T-cells can expand sufficiently in vivo to provide antiviral immunity in the presence of antigen. Other studies used cytolytic T-cell (CTL) lines produced with antigen-

presenting cells which were transduced with AdV vectors. Ultimately, broad implementation of this cell therapy requires the development of T-cell production processes that are rapid, cost-effective, and feasible when starting from small blood volumes. If this can be achieved, T-cell immunotherapies may possibly move beyond highly specialized centers to a standard-of-care therapy available to all [2].

2.6.3 Antiviral drugs for ocular infections

Since no approved antiviral treatment for ocular AdV infections is currently existing, the management of EKC is merely supportive. The possibility for sight-threatening complications warrants the necessity for developing an anti-AdV therapy with superior therapeutic index. AdV is the most common cause of infectious conjunctivitis worldwide; this virus accounts for up to 75% of all conjunctivitis cases and affects individuals at any age and independent of the person's immune status. Outbreaks of EKC are usually caused by AdV-8, -19, -37 and -54. Although this infection of the ocular surface primarily affects the conjunctival surface, AdV may also gain entry into the cornea, inducing innate and cell-mediated immunopathology. Among patients with EKC, common clinical signs are redness, inflammation, eye lid swelling, impaired vision, and pain lasting for two to three weeks [3, 20].

Although AdV conjunctivitis is self-limiting, a few treatment options have been investigated to try to alleviate symptoms or shorten time of infection. The antiviral drugs ganciclovir and cidofovir, which are nucleoside/nucleotide inhibitors of the AdV DNA polymerase, have demonstrated in vitro activity against various AdV types. Unfortunately, small-scale clinical studies with cidofovir eye drops in patients have had a disappointing outcome due to local drug toxicity (i.e. increased ocular pressure and lacrimal canalicular blockade). An antiviral drug that blocks virus entry into the conjunctival or epithelial tissues would be ideal to halt the inflammatory cascade that is typical for EKC disease [7, 20-22].

Topical immunoglobulin (Ig) has proven to work against AdVs in vitro and in vivo, by successfully neutralizing the virus on the ocular surface. Since this intervention acts in an early phase of infection, it could prevent painful symptoms and further virus spread. Though animal studies have demonstrated some success with topical Ig, there is an availability issue which is related to Ig production from serum donors and achieving product consistency. Thus far, data in infected humans are lacking [7, 20-22].
Povidone-iodine, an antiseptic which is often used for sterilization prior to ocular surgery, has broad-spectrum antibacterial, antiviral and antifungal properties. Its use against AdVs is under investigation. Furthermore, corticosteroids like dexamethasone are strong anti-inflammatory products. Their application against AdV infection has been shown to actually prolong viral shedding and inhibit immunological clearance. Other negative effects of prolonged corticosteroid use are glaucoma and cataract formation. For this reason, corticosteroids are often used in combination with other compounds. A recent controlled randomized study was performed with eye drops containing povidone-iodine 1.0% plus dexamethasone 0.1%. Patients on this regimen showed nearly complete recovery of AdV infection in as little as five days [4, 20].

2.7 Experimental compounds

To date, there are no specific antiviral drugs available for the treatment of AdV infections. AdVs are obligate intracellular pathogens that are fully dependent on the cellular replication machinery of their host. The selective inhibition of AdV replication by antiviral compounds is therefore difficult to achieve as some of the essential functions of the host cells may also be altered.

2.7.1 DNA synthesis inhibitors

Ongoing research on anti-AdV activities of nucleoside and nucleotide analogous is aimed at finding derivates with superior activity and safety. As of today, cidofovir and its prodrug brincidofovir are the only compounds which have proven to produce AdV suppression at multiple clinical centers. As already explained, the nephrotoxicity of systemic cidofovir, ocular toxicity of topical cidofovir, and gastrointestinal toxicity of brincidofovir, are drawbacks for their wide use against severe systemic or ocular AdV infections. Besides, a few 2',3'-dedeoxynucleoside analogues developed as HIV inhibitors, proved able of inhibiting AdV DNA synthesis. Among a series of tested analogues, zalcitabine (ddC) and alovudine (FddT) were found to be quite selective AdV inhibitors. These two compounds are potential candidates for systemic and/or topical treatment of AdV infections, and warrant investigation in experimental and clinical studies [1, 3, 6].

2.7.2 Protease inhibitors

The AdV cysteine protease, also called adenain, mediates several critical steps during both early and late stages of virus replication. Adenain supports uncoating of the viral particles during virus entry and processes several capsid and core precursor proteins required for formation of mature infectious virions. It has also been implicated in host cell lysis through cleavage of cytoskeletal proteins. Thus, inhibition of adenain seems a valid treatment strategy for AdV infections such as EKC. Structure-based inhibitor design at the Novartis Institute for Biomedical Research, yielded a few peptidomimetic inhibitors that mimicked the consensus substrate cleavage sites of adenain and contained a nitrile moiety as the electrophilic warhead. This effort resulted in two lead compounds as a suitable starting point for designing adenain inhibitors with improved potency in AdV-infected cells [23].

2.7.3 Entry inhibitors

An attractive approach is to block the initial interaction between the virus and host cell, thereby preventing virus attachment and entry. Whereas non-EKC causing AdVs use mainly CD46 and CAR as receptors, EKC-causing AdVs bind to sialic acid-containing glycans on epithelial cells in the cornea or conjunctiva. Hence, natural or synthetic sialic acid derivatives could be relevant entry inhibitors. An important asset in the context of EKC is related to two unfavorable properties of carbohydrate-based drugs, namely rapid serum clearance and poor cellular uptake after systemic administration. These issues are irrelevant in the case of topical administration (e.g. eye cream, ointment or drops) and an extracellular action point. In order to circumvent the relatively low efficacy of monovalent sialic acid derivatives, the research group of Adenovir Pharma took advantage of the trimeric binding site of the Ad37 fiber knob.

The use of multivalent sialic acid derivatives or glycoconjugates that simultaneously bind several carbohydrate recognition domains per knob considerably improved the inhibitory potency in comparison to the sialic acid monosaccharide [21]. Adenovir Pharma's drug candidates APD-209 and APD-514 Eyedrops are concluded to be safe and well tolerated in several pre-clinical toxicity studies. A multi-center randomized double-masked placebo-controlled Phase 2a clinical study with APD-209 in EKC patients has been completed. The study did not give a conclusive result as the evaluable patients who met the inclusion criteria proved to be too few to show statistically significant efficacy [24].

2.8 Pharmacology of immunosuppressant agents used in the transplantation setting

As explained before, there is no knowledge about which immunosuppressive or cytostatic agents could possibly modulate AdV infection in immunocompromised individuals such as HSCT or organ transplant recipients, or cancer patients receiving chemotherapy. For some conditions (like end-stage renal disease), transplantation represents a life-threatening intervention. The success of transplantation is largely related to continuous efforts to develop better immunosuppressants. Although many new drugs have become available since the landmark discovery of cyclosporin, the risk for AdV or other opportunistic infections is an intrinsic hazard of all current immunosuppressive medications.

As shown on Fig. 5, HSCT patients can receive two kind of therapies. Myeloablative or non-myeloablative stem-cell transplant [25].
Myeloablative allogeneic hematopoietic stem-cell transplantation (panel a in Fig. 5) involves administration of intensive chemotherapy (ovals), often combined with total body irradiation (lightning bolts), before the cells are transplanted (at day 0). Allogeneic hematopoietic stem cells are typically obtained from bone marrow or from the peripheral blood after growth-factor administration. The intensive chemoradiotherapy provides significant antitumor activity, but decreases host hematopoiesis and immunity. Engraftment of donor stem cells (allogeneic hematopoietic stem-cell infusion) is essential to rescue the patient from lethal hematopoietic toxicity. Immunosuppressive drugs, such as cyclosporine and methotrexate, are administered post-transplantation to prevent graft-versus-host disease (GVHD). The main complications of HSCT following this myeloablative regimen are organ damage, due to the intensive cytotoxic therapy, opportunistic infection during the period of profound neutropenia, and GVHD. The intensive chemoradiotherapy and the graft-versus-leukemia (GVL) effect of donor immune cells both contribute to the eradication of the leukemia [25].
During non-myeloablative conditioning (panel b in Fig. 5), fludarabine combined with reduced-intensity chemotherapy or low-dose total-body irradiation, are administered to the patient before the hematopoietic stem cells are transplanted. This less intensive conditioning is not myeloablative, but is sufficiently immunosuppressive to allow engraftment of donor stem cells. Immunosuppressive drugs such as cyclosporine and mycophenolate mofetil are administered both to prevent rejection of the transplanted donor cells and to prevent GVHD. The main complications of stem- cell transplantation following this non-myeloablative regimen are GVHD and opportunistic infections that occur as a consequence of immunosuppressive therapy. The GVL effect that is mediated by donor immune cells is solely responsible for the eradication of the leukemia [25].

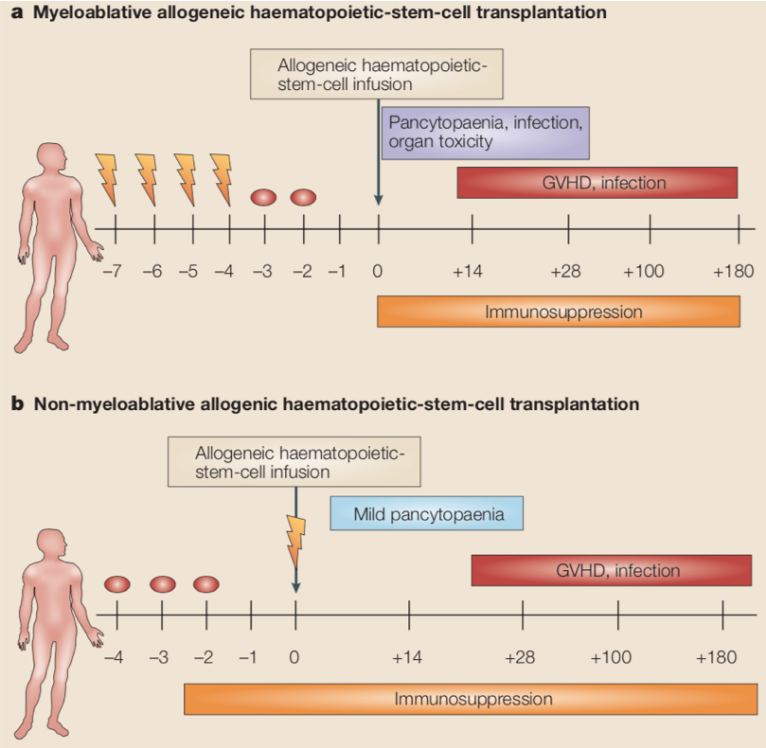

Figure 5. Myeloablative and non-myeloablative stem-cell transplant. Source: Bleakley *et al*. [25]

In the next section, the action principle of commonly used immunosuppressant (see summarizing Fig. 6 and cytostatic drugs will be explained, particularly those included in this investigation. Extra attention is given to the mTOR inhibitor sirolimus to introduce the anti-AdV mechanistic studies that are performed in this thesis.

2.8.1 Calcineurin inhibitors

The calcineurin inhibitors (CNIs) ciclosporin (cyclosporin A) and tacrolimus are fungus-derived cyclic peptides. They are the mainstay of current maintenance immunosuppressive regimens and inhibit the synthesis of interleukin-2 (IL-2). After the CNIs bind to cytoplasmatic proteins called immunophilins, the immunophilin-drug complex inhibits the activity of calcineurin, a serine phosphatase that normally dephosphorylates nuclear factor of activated T-cells (NFAT) resulting in nuclear translocation of this factor and transcription of IL-2. This cytokine has an important role in activation and proliferation of T-lymphocytes, hence CNIs are potent anti-T-cell agents.

CNIs show many CYP3A4- and P-glycoprotein-related drug interactions and may produce some serious side effects. In individuals with hypertension hyperlipidemia and increased risk of rejection, tacrolimus seems preferred whereas ciclosporin is favored in those with a high risk of new-onset diabetes [26].

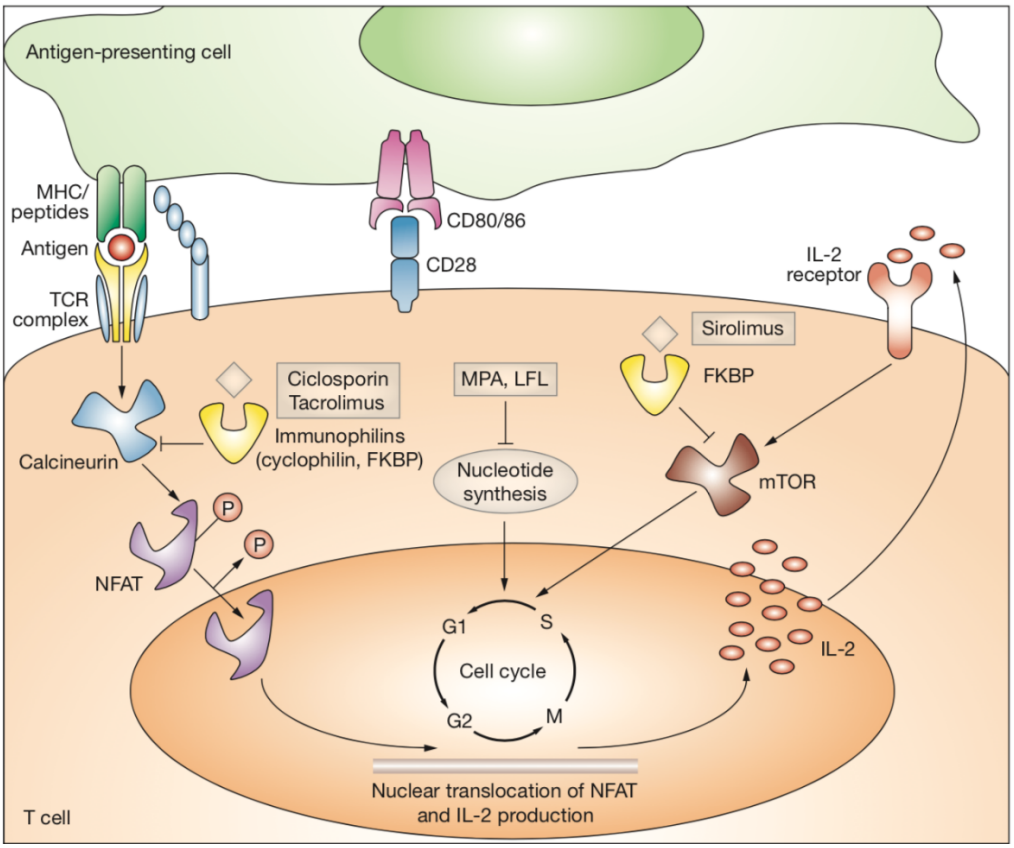

Figure 6. Mechanisms of action of maintenance immunosuppressive agents. CNIs (ciclosporin and tacrolimus) bind to their respective immunophilins, and inhibit calcineurin. Calcineurin is then unable to dephosphorylate NFAT, which will prevent translocation of NFAT to the nucleus and thereby production of IL-2. Sirolimus is an mTOR inhibitor. It binds to FKBP and inhibits mTOR, which in turn inhibits transition of the cell cycle from G1 to S phase. MPA and LFL are also cell-cycle inhibitors, and act via inhibition of nucleotide synthesis. Abbreviations: CNI, calcineurin inhibitor; FKBP, FK506-binding protein; IL-2, interleukin-2; LFL, leflunomide; MHC, major histocompatibility complex; MPA, mycophenolic acid; mTOR, mammalian target of rapamycin; NFAT, nuclear factor of activated T-cells; TCR, T-cell receptor. Source: Samaniego *et al.* [26].

2.8.2 Inhibitors of the mammalian target of rapamycin

The mammalian target of rapamycin (mTOR) is a central regulator of gene expression, translation and various metabolic processes. Multiple extracellular (growth factors) and intracellular (energy status) signals as well as a variety of stressors come together into the mTOR pathway. Virus infection is a significant stress factor that can activate, reduce or even suppress the mTOR signaling pathway. Consequently, viruses have evolved a plethora of different mechanisms to attack and co-opt the mTOR pathway in order to make the host cell a hospitable environment for their replication [27].

Sirolimus and its derivative everolimus are macrolide immunosuppressants isolated from Streptomyces hygroscopicus. They bind to the immunophilin FK-binding protein 12 (FKBP12) which is also targeted by tacrolimus. The sirolimus-FKBP12 and everolimus-FKBP12 complexes inhibit mTOR, resulting in inhibition of lymphocyte proliferation and cell cycle arrest at the G1 phase [26].

Sirolimus is metabolized by CYP3A4 and P-glycoprotein. Sirolimus and ciclosporin were found to have similar efficacy in preventing acute rejection, but different safety profiles. Sirolimus appears useful to minimize the use of CNIs in select patient populations [26].

2.8.3 Cytostatic agents

The antiproliferative agents described below inhibit the proliferation of activated immune cells by interfering with different aspects of DNA or RNA synthesis.

Mycophenolic acid (MPA) is the active metabolite of mycophenolate mofetil (MMF) and enteric coated mycophenolate sodium (MPS). MPA is a noncompetitive and selective inhibitor or inosine monophosphate dehydrogenase, the rate-limiting enzyme in the de novo pathway of purine synthesis. Inhibition of this enzyme prevents proliferation of activated T- and B-cells. MFF and MPS have similar adverse-effects, like gastrointestinal toxicity and bone marrow suppression [26].
Leflunomide (LFL) and its analog FK778 inhibit the activity of dihydroorotate dehydrogenase, a rate limiting enzyme in de novo pyrimidine biosynthesis. It prevents lymphocytes from producing sufficient pyrimidines to support DNA synthesis. Its use can produce gastrointestinal adverse effects, bone marrow suppression and severe hepatitis [26].

3. Materials and methods

First, the cell lines, AdV stocks, antiviral compounds, immunosuppressive agents, primers and antibodies used for experiments are described. Next, the methods used in this project and their optimization are described in detail.

3.1 Cells and media

Three different cell lines were tested during experimental research. Human embryonic lung (HEL) cells and human lung carcinoma A549 cells were purchased from American Type Culture Collection (ATCC) (# CCL-137 and # CCL-185, respectively). Whereas HEL cells have a limited growing capacity and must be used within ten passages, A549 cells are a continuous cell line that is cancer-derived. Both cell lines show clear and microscopically visible cytopathic effect (CPE) when infected with AdV. CPE means that the infecting virus causes lysis of the host cell or when the cell dies without lysis due to an inability to reproduce.
The 293AD cells were purchased from Cell Biolabs (# AD-100). This cell line was selected from HEK293 cells, a human embryonic kidney cell line that contains the AdV-5 E1 region and is widely used to propagate E1-deleted AdV vectors. Whereas HEK293 cells show poor adherence to culture plastic, 293AD cells show a flattened morphology and firm attachment, which makes them more suitable for further antiviral studies.
The HEL, A549 and 293AD cells were subcultivated in 75-cm^2 flasks in Dulbecco's Modified Eagle Medium 1x (DMEM 1x) supplemented with 8% heat-inactivated fetal calf serum (HI-FCS), 1 mM sodium pyruvate and 750 mg per L sodium bicarbonate.
HEL cells were passaged once per week; the other two cell lines twice per week. The cells were washed with phosphate-buffered saline (PBS), then detached from the plastic using 0.25% (w/v) trypsin-0.53 mM ethylenediamine tetraacetic acid (EDTA). After 2-5 minutes incubation at 37 °C, the cells were resuspended in medium and transferred to new flasks to achieve a split ratio of 1/2 (HEL) or 1/10 (A549 and 293AD).

During virus experiments, infection medium was used, consisting of DMEM 1x supplemented with 2% HI-FCS, 1 mM sodium pyruvate and 750 mg per L sodium bicarbonate. The A549 cells were counted to ensure reproducible cell density in the plates. [This was not done for HEL cells, since these cells show profound contact inhibition and are difficult to count which is related to their flattened morphology.] Ten µL of the A549 cell suspension was mixed with 10 µL of trypan blue solution. Next, 10 µL was pipetted into a LUNA™ cell counting slide and read in a LUNA-II™ Automated Cell Counter (Logos Biosystems). The A549 cells were seeded into 96-well plates one day prior to virus infection at a density of 2,500 cells per 100 µL per well. HEL cells were seeded one week before use in a volume of 200 µL per well to prevent drying out. One 75-cm^2 flask with confluent HEL cells was used to prepare about fifteen 96-well plates.
All cell flasks and plates were incubated in a humidified 5% CO_2 incubator at 37°C.

3.2 Virus stocks and AdV hexon sequencing

The following five human AdVs were purchased from ATCC: AdV-2 (subgroup C; strain Adenoid 6; # VR-846); AdV-3 (subgroup B; strain GB; # VR-3); AdV-7 (subgroup B; strain Gomen); AdV-8 (subgroup D; strain TRIM) and AdV-9 (subgroup D; strain HICKS). To make virus stocks, an aliquot of the ATCC stock was added to confluent A549 cells in 25-cm^2 flasks, incubated for 3-8 days until about 75% CPE was visible, then frozen at -80°C. To prepare the virus stock, the flask was rapidly thawed and cell lysates were clarified by centrifugation (4°C, 20 min, 1800 *g*). Finally, the stock was aliquoted in cryotubes and stored at -80 °C.
The green fluorescent protein (GFP)-expressing AdV-5 vector deleted in E1 and E3 regions was purchased from GenTarget (# AVP011). This virus was propagated in 293AD cells using the same procedure as above.

To quantify the AdVs stocks, virus titers were calculated on both cell lines. For virus titration, 1/10 dilutions of the stocks were added to 96-well plates containing confluent cultures of HEL, A549 or 293AD cells (8 wells per dilution). Once that clear CPE was visible [typically at day 6-10 post infection (p.i.) for A549 cells and day 10-14 p.i. for HEL cells], the plates were scored microscopically and virus titers were calculated by the method of Reed and Münch [28]. This is elaborated in the Results section.

The correct identity of the AdV stocks was verified by sequencing a short part of the AdV hexon DNA. The two universal primers recognize conserved sequences of the AdV hexon DNA, while the 301-bp amplicon shows sufficient sequence differences to allow AdV typing [29]. Virus (500 µL) was added to A549 cells in 12-well plates, and 4 h later, medium was aspirated and cells were washed with PBS. Next, the cells were lysed with AL buffer (Qiagen), scraped off and collected into tubes to store at -20°C. From these cell lysates, total cellular DNA extracts were prepared using the QIAamp DNA Mini Kit (Qiagen) following the manufacturer's instructions. The samples were submitted to high fidelity PCR (Invitrogen Platinum Superfi PCR master mix) using the Adeno hexon forward (FW) and Adeno hexon reverse (RV) primers (Table 2).

Table 2. Primer sequences used for PCR.

Primer code	Sequence (5'→3')	T_m (°C)	% GC
Primers for hexon sequencing (amplicon: 301 bp)			
Adeno hexon FW	GCCSCARTGGKCWTACATGCACATC	62.4	56
Adeno hexon REV	CAGCACSCCICGRATGTCAAA	61.8	55
Primers for virus quantification (amplicon: 137 bp)			
Adeno qPCR FW	CGCTGGACATGACTTTTGAG	57.6	50
Adeno qPCR REV	GAACGGTGTGCGCAGGTA	61.1	61

Initially, three different annealing temperatures were compared. The PCR program consisted of an initial denaturation step (30 s at 98°C); 35 or 40 cycli of denaturation (10 s at 98°C), annealing (10 s at 54, 56 or 58°C) and extension (1 min at 72°C); and final extension step of 5 min at 72°C. To check the amplicon size, a small part of the PCR product was analyzed by electrophoresis on a 1% and 2% agarose gel. Samples giving one single band of the correct size were submitted to DNA purification (Wizard® SV Gel and PCR Clean-Up System kit) and after determining the DNA concentration and adding the primers for hexon sequencing, the samples were sent to Macrogen for sequencing. The retrieved DNA sequences were analyzed by BLAST (see Results).

3.3 Test compounds

The test compounds used for antiviral experiments (see Table 3, 4, 5 and 6 for detailed list) fall into four categories: (1) inhibitors of viral polymerases; (2) inhibitors of virus entry; (3) immunosuppressive and immunomodulatory compounds; and (4) cytostatic agents.

Table 3. List of test compounds and their working mechanisms [30].

Inhibitors of viral polymerases	
Cidofovir (CDV)	Broad DNA-virus inhibitor; approved for CMV therapy
Alovudine (FddT)	Inhibits HIV reverse transcriptase; development halted during clinical trials
Zalcitabine (ddC)	Inhibits HIV reverse transcriptase; approved for HIV therapy
Ribavirin (RBV)	Broad DNA- and RNA-virus inhibitor; approved for RSV infection, hepatitis C virus, and viral hemorrhagic fever
Trifluorothymidine (TFT)	Herpes virus inhibitor; approved as eye drops for ocular herpes virus infections
Vidarabine (Ara-A)	Herpes virus inhibitor; approved for systematic herpes virus (discontinued)
Experimental inhibitors of virus entry	
$NMSO_3$	Sulfated sialyl lipid compound with broad antiviral activity
Dextran sulfate (DS-10,000)	Polyanionic compound with broad antiviral activity
Wheat germ agglutinin lectin (WGA)	Sialic acid-binding lectin compound; acts against sialic acid-dependent viruses
Hippeastrum hybrid agglutinin (HHA)	Mannose specific lectin with broad antiviral activity
Galanthus nivalis agglutinin (GNA)	Mannose specific lectin with broad antiviral activity

Urtica dioica agglutinin (UDA)	Mannose specific lectin with broad antiviral activity
Pradimicine-S (PRM-S)	Mannose-binding antibiotic from natural source; with broad antiviral and antifungal activity
Immunosuppressive and immunomodulatory agents	
Cyclosporin	Calcineurin inhibitor; blocks IL-2 synthesis and lymphocyte proliferation; used to inhibit transplant rejection
Tacrolimus	Calcineurin inhibitor; blocks IL-2 synthesis and lymphocyte proliferation; used to inhibit transplant rejection
Sirolimus	Inhibits the mTOR pathway; blocks signal transduction pathways and lymphocyte proliferation; used to inhibit transplant rejection
Imiquimod	TLR7 agonist; used against recurrent genital warts
Mycophenolic acid (MPA)	IMP dehydrogenase inhibitor Inhibits lymphocyte proliferation
Leflunomide	Inhibitor of pyrimidine synthesis and protein kinase activity; used to inhibit transplant rejection and potentially for CMV therapy
Cytostatic molecules	
Gemcitabine	Pyrimidine antagonist Chain terminator when incorporated into DNA
Cytarabine (Ara-C)	Pyrimidine antagonist Chain terminator when incorporated into DNA
9-(2-Phosphonylmethoxyethyl) guanine (PMEG) (not approved)	Purine antagonist Chain terminator when incorporated into DNA
5-Fluorouracil (5-FU)	Pyrimidine antagonist Chain terminator when incorporated into DNA
Cladribine	Purine antagonist Inhibits ribonucleotide reductase
Clofarabine	Purine antagonist Approved for acute myeloid leukemia
Fludarabine	Purine antagonist Interferes with duplication of DNA
Methotrexate	Binds to dihydrofolate reductase and interferes with thymidylate synthesis
Decitabine	Inhibitor of DNA methyltransferase Inhibits lymphocyte proliferation
Azacitidine	Inhibitor of DNA methyltransferase Inhibits lymphocyte proliferation
Imatinib	Tyrosine kinase inhibitor Inhibits Bcr-Abl kinase, c-kit kinase

3.4 Flow cytometric analysis of virus receptor expression

To determine the expression of CD46 and CAR, two well-known AdV receptors, a Fluorescence-Activated Cell Sorting (FACS) analysis was performed on the cell lines used in this study.

Cells grown in 75-cm^2 flasks were detached using different reagents [i.e. non-enzymatic cell dissociation buffer (Sigma-Aldrich) or 0.25% trypsine-EDTA; see Results] and counted. Depending on these reagents, an incubation stage in cell culture medium was performed to allow the detached cells to repair their surface receptors. A cell suspension containing 250,000 cells per 100 μL was transferred to each FACS tube and centrifugated at 1200 RPM for 10 min. Then, the cells were washed two times with FACS buffer (i.e. PBS plus 2% FCS) by discharging the supernatants and resuspending the pellets in FACS buffer.

As control for non-specific background staining, a condition was included that was stained with an isotype control antibody (from BD Biosciences), to reduce aspecific binding. The cells were incubated in 100 μL FACS buffer with 2.5 μg of Human BD Fc Block for 10 minutes at room temperature, followed by staining with the desired fluorescent antibody. No washing step was needed between the blocking and staining steps.

In the companies' recommendations, 1 μg antibody was advised per 10^6 cells, which corresponded to 5 μL antibody per FACS tube. In this experience, much less antibody proved to be sufficient (see Results). The antibodies used are listed in Table 7. After 30 min incubation in the dark, the cells were washed with 2 mL FACS buffer, then centrifugated at 1200 RPM for 10 min. The supernatants were discharged and the pellets were resuspended in 250 μL Fixation Solution (PBS plus 1% formaldehyde).

Finally, the cells were analyzed on a Becton-Dickinson FACSCelesta Flow Cytometer, using FlowJo software for data analysis.

Table 4. Antibodies used for FACS analysis of AdV receptor expression.

Antibody code	Company	Description	Dilution
Detection of CAR			
SC-56892	Santa Cruz Biotechnology	Anti-CAR antibody: mouse monoclonal antibody (clone E1-1); labeled with phycoerythrin (PE)	Non-diluted; 1/20;1/100; 1/500; and 1/1000
SC-2868	Santa Cruz Biotechnology	Control antibody: Isotype IgG2b; labeled with PE	
Detection of CD46			
FAB2005R	R&D systems	Anti-CD46 antibody: mouse monoclonal IgG2b antibody (clone 344519); labeled with Alexa Fluor 647	Non diluted 1/20, 1/100, 1/500 and 1/1000
IC0041R	R&D systems	Control antibody: Isotype IgG2B (clone 133303) labeled with Alexa Fluor 647	

3.5 Antiviral evaluation by CPE reduction assay

The compounds were evaluated in three independent experiments. HEL and A549 cells were seeded in 96-well plates (see section 3.1 page 31) On the day of virus infection, culture medium was aspirated and replaced by 100 µL infection medium in each well. Next, the test compounds were added by pipetting 25 µL of a compound stock solution at 1000 µM, to the 100 µL infection medium, thus yielding a compound concentration of 200 µM. A dilution series was made by pipetting 25 µl to the next well, until a row of eight dilutions was achieved for every compound. Next, 100 µL diluted AdV was added to each well, meaning that the final compound concentrations were reduced to half. Every plate contained six wells receiving no compound (= virus control) and six wells receiving no compound and no virus (= cell control). In one parallel plate, no AdV was added to allow assessment of the compounds' cytotoxicity. Finally, all plates were incubated at 37°C.

After 8-12 days incubation at 37 °C, virus-induced CPE and compound cytotoxicity were scored by microscopy. The microscopic CPE scores (i.e. score 0, 1, 2, 3 or 4 corresponding to 0, 25, 50, 75 or 100% of the cells being lysed by the virus) in compound-treated virus-infected cells were expressed relative to the virus control set at 100%. From these values, the compound's antiviral 50% effective concentration (EC_{50}) was calculated by interpolation, based on a semilog dose-response curve. Compound cytotoxicity was expressed as the MCC (minimal cytotoxic concentration), i.e. the minimal test concentration producing visible alterations like rounding, shrinking or lysis of the cells.

The cells were next submitted to the MTS assay, a colorimetric method for sensitive quantification of cell viability. It is based on conversion of a yellow reagent into a brown formazan product; only viable cells are able to perform this metabolic reaction. To perform the test, the MTS cell viability reagent (CellTiter 96® AQueous MTS Reagent from Promega) was added to the 96-well plates, and 2 h later, absorbance at 490 nm was recorded in a Molecular Devices SPECTRAmax plus 384 plate reader. The recorded optical density (OD) values were used for the following calculations. The % protection against virus was defined as: [(OD_{Cpd})virus - (OD_{Contr})virus)] / [(OD_{Contr})cells - (OD_{Contr})virus] x 100, where (OD_{Cpd})virus is the OD for a given concentration of the compound in virus-infected cells; (OD_{Contr})virus is the OD for the virus control; and (OD_{Contr})cells is the OD for the cell control. The % cytotoxicity was defined as: [1 - (OD_{Cpd})cells / [(OD_{Contr})cells] x 100, where (OD_{Cpd})cells is the OD for a given concentration of the compound in mock-infected cells. Based on these % protection and % cytotoxicity values, the compound's EC_{50} and CC_{50} (50% cytotoxic concentration) values were derived by interpolation, based on a semilog dose-response curve.

3.6 Antiviral evaluation by qPCR quantification of virus yield

To verify the compounds' inhibitory effect on AdV replication, the AdV virus yield in the supernatant was quantified, using an established qPCR method [6]. The HEL cells were infected with AdV and treated with compounds as above, and at day 12 p.i., the supernatants (SN) of HEL cells infected with AdV-2 were frozen in PCR tubes at -80 °C.

Two µl of each harvested supernatant was mixed with 10 µl resuspension buffer and 1 µl lysis reagent (CellsDirect One-Step qRT-PCR kit; Invitrogen) to disrupt the virus particles. After 10 min heating at 75°C, 2 µl of lysate together with 23 µl reaction mix (see Table 8) were pipetted into each well of the PCR plate. To allow absolute quantification, a dilution series was included of a PCR standard, consisting of a pGEM T-vector containing a 691-bp fragment of AdV hexon DNA. All samples were run in duplicate.

Table 5. Reaction mix for one sample for qPCR analysis of AdV DNA copy number.

Reaction mix for 1 sample:	volume		concentration
GoTaq qPCR MM (2X)	12.5	uL	1X
Forward Primer (25 uM)	0.3	uL	0.3 uM
Reverse Primer (25 uMX)	0.3	uL	0.3 uM
Nuclease Free Water	9.9	uL	/
Total reaction mix volume:	**23**	**uL**	
DNA sample volume:	**2.0**	**uL**	

The qPCR program was performed on an ABI 7500 Fast Real-Time PCR apparatus (Applied Biosystems) and consisted of: 10 min initial denaturation at 95°C and 40 thermal cycles of 15 sec at 95°C and 60 sec at 60°C, followed by a dissociation stage to verify that only one DNA product was formed.
The two primers (see Table 2) amplified a conserved human AdV hexon DNA sequence of 137 bp. The C_t-values obtained with the diluted plasmid standard were used to draw a standard curve (R^2 >0.98 within the range of 10^3 to 10^8 copies per reaction), this standard curve was used to convert the C_t-values for the extracts into the absolute number of human AdV DNA.
The EC_{99} and EC_{90} values were calculated by interpolation and defined as the compound concentration causing respectively a 2-$\log_{10}$ and 1-$\log_{10}$ reduction in DNA copy number, as compared to the virus control receiving no compound.

3.7 Fluorescence microscopy for monitoring replication of GFP-encoding AdV-5 vector

The AdV-5 vector AVP011 is a GFP-encoding AdV-5 virus that is deleted in the E1 and E3 regions. This virus shows productive replication (i.e. with release of new vector particles in the medium) in 293AD cells since these cells show constitutive expression of the AdV-5 E1 proteins. On the other hand, when AVP011 is added to HEL or A549 cells, replication is abortive giving a prominent GFP signal but no formation of vector particles.

To monitor the GFP signal, the cells were seeded in 96-well plates and infected with serial dilutions of AVP011. The plates were transferred to an Incucyte instrument (Essen BioScience) set at 37 °C and photographs were taken at 1 hour intervals.

3.8 ELISA assay for detection of mTOR activation

A commercially available ELISA kit (Abcam ab168538) was purchased to quantify mTOR activation and potential effect of AdV infection or compound exposure on this pathway. The kit includes a phosphospecific (pSer2448) anti-mTOR antibody. Since a positive control was required to validate correct use of the kit, protein extracts were prepared from cells undergoing 48 h serum starvation, followed by mTOR activation by exposing the cells to DMEM 1x medium supplemented with either (i) 20% HI-FCS for 1 h; (ii) 2 mM L-glutamine for 1 h; or (iii and iv) 50 nM calyculin A for 15 or 30 min. The action mechanism of these mTOR activators is shown in Fig. 7 [31]. Calyculin A, not mentioned on this scheme and an inhibitor of some protein phosphatases, is recommended as a positive control in the datasheet of the pruchased ELISA kit.

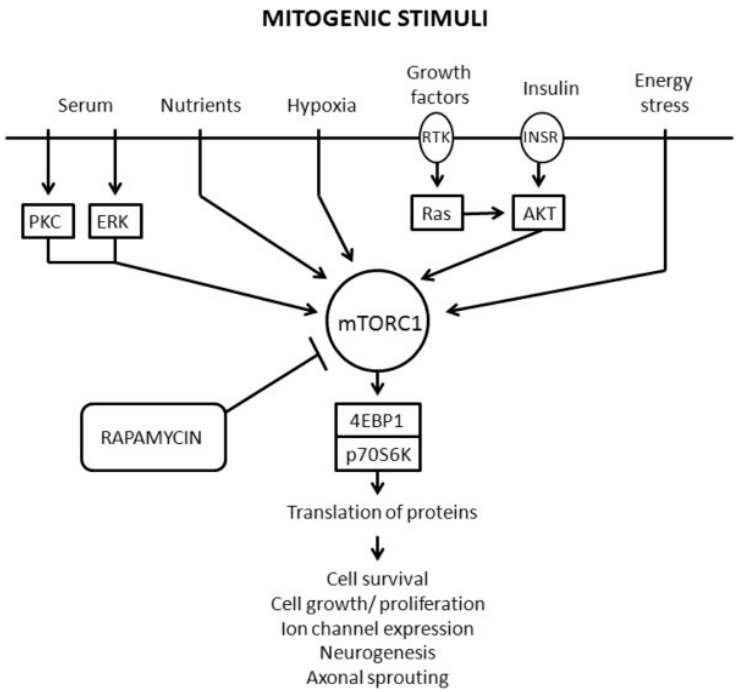

Figure 7. Concise scheme of the mTOR signaling pathway and its activators. mTORC1 receives and integrates the signals from various upstream pathways, including pathways triggered by nutrients, growth factors, hypoxia and insulin that promote cell growth, division and differentiation. Sirolimus (also called rapamycin) is a powerful inhibitor of mTORC1 activity. Abbreviations: 4E-binding protein 1 (4EBP1); eukaryotic translation initiation factor 4E (eIF4E); receptor tyrosine kinase (RTK); insulin receptor (INSR); protein kinase C (PKC); extracellular signal regulated kinase (ERK); small GTPase protein (Ras); Protein kinase B (AKT or PKB). Source: Sharon *et al.* [32].

The mammalian target of rapamycin (mTOR) is a highly conserved serine-threonine kinase that is essential for the coordination of intra- and extracellular signals concerning cell growth, division and differentiation. It is found in two complexes within the cell: mTORC1 and mTORC2, which act upstream of the complex mTOR pathway. mTORC1, responsible for coordinating growth factor-dependent growth and proliferation, becomes active in response to various upstream signals such as growth factors and nutrients (summarized in Fig. 7) and is inhibited by the natural macrolide compound rapamycin, also known as sirolimus [32].

Phosphorylation of mTOR at Ser2448 is carried out directly by AKT kinase, as well as by p70S6 kinase acting as feedback signal. Phosphorylation at this Ser2448 site is a biomarker for activation state of the PI3K pathway as well as the activation status of mTOR.

The ELISA kit was tested for measurement of phospho-Ser2448 mTOR protein in serum-starved cells boosted with FCS (which is rich of growth factors), L-glutamine or the phosphatase inhibitor calyculin A. To prepare cell extracts, the cells were washed three times with PBS, then treated with 750 µl extraction buffer supplemented with Halt® protease and phosphatase inhibitor mix (both from Thermo Fisher Scientific) per well. Following Bradford analysis of total protein concentration, samples containing equal (i.e. 55 µg) amounts of total protein were transferred to one strip of the ELISA plate. Next, the manufacturer's instructions were followed for staining with a prepared director antibody alongside a prepared horseradish peroxidase (HRP) label with HRP development solution was added. Finally, the strip was read in a SPECTRAmax plus 384 plate reader (Molecular Devices) to quantify the absorbance (450 nm) signal.

4. Results and discussion

4.1 Titration and sequencing of the AdV stocks

In this project, a series of diverse compounds against several AdV types were evaluated. First, to ensure that all AdVs were tested at similar stringency, careful titration of the virus stocks was required. The end-point dilution method was used to determine these virus titers expressed as cell culture-infective dose 50% ($CCID_{50}$). Serial dilutions of the virus stocks were prepared and added in eight-fold to HEL or A549 cells. After a few days, the AdV-induced CPE (visible as cell lysis over the entire monolayer or in distinct plaques) was scored by microscopy and the wells were scored with a '+' (denoting that one or more plaques were observed) or '-' (denoting that the cells looked perfectly healthy). An example of the calculation method (originally developed by Reed and Münch [28]) is shown in Fig. 8. At the end, the calculation yields the virus stock dilution corresponding to 1 $CCID_{50}$, from where the titer of the virus stock is derived. In this example, the virus stock has a titer of 3,831,187 $CCID_{50}$. Since, in the antiviral experiments, a 'multiplicity of infection' of 100 $CCID_{50}$ is wanted, a virus dilution of 1/38,312 is needed, which is rounded to 1/40,000.

1) Column B : fill in the dilution series.
2) Column D: for each dilution, fill in the number of wells showing CPE.
3) Column E: for each dilution, fill in the number of wells showing NO CPE.
4) Columns F-G-H: are calculated automatically.
5) Column I gives the percentage positivity for each dilution.

A	B	C	D	E	F	G	H	I
Dilution		Log dilution	Sum of pos.	Sum of neg.	Acc. pos.	Acc. neg.	Total	Perc. pos.
1/	10	1	6	0	37	0	37	100,00
1/	100	2	6	0	31	0	31	100,00
1/	1000	3	6	0	25	0	25	100,00
1/	10000	4	6	0	19	0	19	100,00
1/	100000	5	6	0	13	0	13	100,00
1/	1000000	6	6	0	7	0	7	100,00
1/	10000000	7	1	6	1	6	7	14,29
1/	100000000	8	0	6	0	12	12	0,00

6) In the small table, fill in the dilutions and percentage of positivity around the 50% value.
7) The CCID50 is calculated by 1/ 10^log of CCID50 dilution.

	Log dilution	Perc. pos.
>50% result	6	100
<50% result	7	14,29

Log of CCID50 dilution =	**6,583333333**	CCID50 dilution = 1/	3831186,85

Figure 8. Example of the method to calculate the virus titer expressed in $CCID_{50}$.

In Table 6, the working dilutions of the different AdV stocks for HEL and A549 cells are summarized. It can be noticed that the AdVs require a more diluted virus for the A549 compared to HEL experiments. A possible explanation is that AdV replication is much more efficient in A549 than HEL cells, which is likely related to the fact that HEL cells are very slow growing cells. This is also evident from the observation that AdV CPE develops faster in A549 cells (between 6-10 days p.i.) compared to HEL cells (between 10-14 days p.i.).

Table 6. Virus stock dilutions for the different AdV types and for HEL and A549 cells.

Virus stocks	Dilutions for HEL	Dilutions for A549
AdV-2 (ATCC VR846)	1/1,500	/
AdV-2 (ATCC VR846 diluted)	/	1/4,000
AdV-3 (Ad1_10)	1/250	1/40,000
AdV-7 (Ad1_11	1/250	1/25,000
AdV-8 (Ad1_15)	1/250	1/80,000
AdV-9 (Ad1_13)	1/1,500	1/25,000

Besides virus quantification, a qualitative analysis on the AdV stocks was performed to verify their correct identity. This was done by sequencing a short part of the AdV hexon DNA, using a pair of universal primers (see Table 2 in Materials and Methods). It was first verified that these primer sequences are indeed highly conserved among AdV types (Fig. 9), by making an alignment of hexon sequences found in literature. The forward primer (purple) and reverse primer (blue) show only a few mismatches, while the 301-bp amplicon that is delineated by these two primers shows sufficient sequence differences to allow AdV typing.

```
AdV8(AB330089.1)    CAACTCGGCGCACGCGCTCGACATGACCTTTGAGGTGGACCCCATGGATGAGCCCACCCT
AdV9(AB330090.1)    CAACTCGGCCCACGCGCTCGACATGACCTTCGAGGTGGACCCCATGGATGAGCCCACCCT
AdV3(AY854178.1)    CAACTCAGCCCATGCGCTGGACATGACTTTTGAGGTGGATCCCATGGATGAGCCCACCCT
AdV7(AB330088.1)    CAACTCAGCCCATGCGCTGGACATGACTTTTGAGGTGGATCCCATGGATGAGCCCACCCT
AdV2(AB330083.1)    CAACTCCGCCCACGCGCTAGACATGACTTTTGAGGTGGATCCCATGGACGAGCCCACCCT
                    ****** ** ** ***** ******** ** ******** ******** ***********

AdV8(AB330089.1)    CCTGTATCTTCTCTTTGAAGTTTTCGACGTGGTCAGAGTGCACCAGCCGCACCGCGGCGT
AdV9(AB330090.1)    CCTCTATCTTCTCTTCGAAGTTTTCGACGTGGTCAGAGTGCACCAGCCGCACCGCGGCGT
AdV3(AY854178.1)    GCTTTATCTTCTTTTCGAAGTCTTCGACGTGGTCAGAGTGCACCAGCCACACCGCGGCGT
AdV7(AB330088.1)    GCTTTATCTTCTTTTCGAAGTCTTCGACGTGGTCAGAGTGCACCAGCCACACCGCGGCGT
AdV2(AB330083.1)    TCTTTATGTTTTGTTTGAAGTCTTTGACGTGGTCCGTGTGCACCAGCCGCACCGCGGCGT
                     ** *** ** * ** ***** ** ********* * ********** **********

AVd8(AB330089.1)    CATCGAGGCCGTCTACCTGCGCACGCCCTTCTCCGCCGGCAACGCCACCACCTAA
AdV9(AB330090.1)    CATCGAGGCCGTCTACCTGCGCACGCCCTTCTCCGCCGGCAACGCCACCACCTAA
AdV3(AY854178.1)    CATCGAGGCCGTCTACCTGCGCACACCGTTCTCGGCCGGCAACGCCACCACATAA
AdV7(AB330088.1)    CATCGAGGCCGTCTACCTGCGCACACCGTTCTCGGCCGGCAACGCCACCACATAA
AdV2(AB330083.1)    CATCGAGACCGTGTACCTGCGCACGCCCTTCTCGGCCGGCAACGCCACAACATAA
                    ******* **** ********** ** ***** ************** ** ***
```

Figure 9. Alignment of AdV hexon sequences published in the literature, with the two universal primers used for the sequencing method marked in color.

The two primers were used for PCR amplification on the five AdV stocks used in this project. The PCR reaction was done at three different annealing temperatures, i.e. 54, 56 and 58 °C. To check the amplicon size of 301 bp, a fraction of the PCR product was analyzed by electrophoresis on a 2% agarose gel. Hardly any difference was seen for the three temperatures (Fig. 10) and all PCR products yielded only one band of the correct size. Therefore, a temperature of 56°C was chosen for further PCR reactions. Unfortunately, for AdV-8 no bands appeared, indicating that the virus titer in this stock was too low. For future experiments, an alternative cell line than A549 is needed to prepare AdV-8 stocks of sufficient strength.

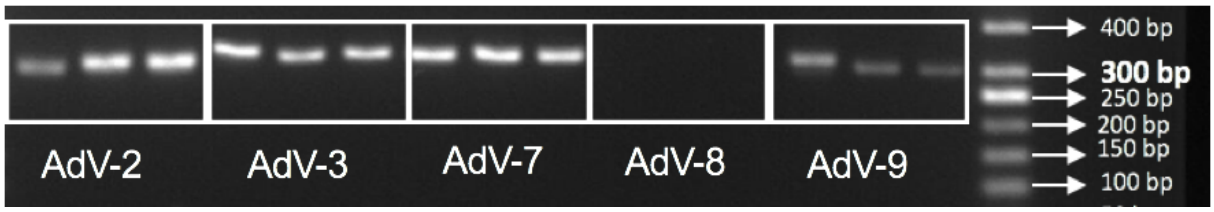

Figure 10. Gel electrophorese of PCR amplicons from each AdV stock at different annealing temperatures. For each AdV type, the order of the different temperatures used is, from left to right, 54, 56 and 58°C.

For the other four AdVs, the PCR products were purified and sent to Macrogen for DNA sequencing. The retrieved DNA sequences, analyzed by BLAST (Table 7), confirmed that each AdV stock was correct, giving a match of 98-99% with the published DNA sequence for this AdV type or strain. To conclude, the reliability was confirmed of the AdV stocks prepared in this project, and established that this sequencing method is useful for quality control on new AdV stocks prepared in the future.

Table 7. Percentage identity of the different AdV stocks compared to published AdV hexon sequences.

Virus stock	Percentage identity to known human AdV	ID of known human AdV sequence
AdV2	99% AdV2	EU128938.1
AdV3	98% AdV3 (GB)	AB330084.1
AdV7	98% AdV7 (Gomen)	AB330088.1
AdV9	98% AdV9 (Hicks)	AB330090.1

4.2 Receptor expression on the different cell lines

Since receptor usage by AdVs is quite heterogeneous, depending on AdV type and cell line, receptor expression was verified of two major AdV receptors, CD46 and CAR, on the cell lines used in this project. This required optimization of the sequential steps for sample preparation, receptor staining and FACS detection. Table 8 is providing a summary of the experimental variations that were tested to finally reach a useful FACS result.

Table 8. Overview of the experimental variations to reach a useful FACS result.

Method	Observation	FACS result
Cells detached with 'cell dissociation buffer'	Cells did not detach from plastic surface	No FACS result
Cells detached with 0.25% trypsine-EDTA	Cells needed 1 h incubation in growth medium to recover cell surface receptors	Good results
Addition of a blocking step with 2.5 μg of Human BD Fc Block	This blocking step gave no difference, and was not further used.	This blocking is not necessary.
Different antibody dilutions were compared	For CD46, even low antibody concentrations were effective.	The method works for CD46.

The FACS results were analyzed with FlowJo software to obtain histograms for visualization of the receptor expression on the different cell lines. As shown in Figs. 11, 12 and 13, also this data analysis required some adjustments.
Fig. 11 shows the result for HEL cells. In case of CD46 staining, the peak showed a clear shift compared to the control stained with isotype. Hence, this AdV receptor is abundantly expressed on HEL cells. With the anti-CD46 antibody, much higher dilutions than recommended by the manufacturer can be used in a cost-effective manner. For CAR, no significant CAR staining was seen, since the peaks for anti-CAR antibody and isotype controls showed complete overlap. Moreover, also the control cells undergoing no antibody staining at all, yielded an overlapping peak. Other dilutions of the anti-CAR antibody did not produce a better result.

The histogram peaks were normalized to mode, which is common in FACS data presentation comparing different population sizes. For histograms, height differences based on absolute cell numbers can create a visual bias. Therefore, %max scaling in histograms is achieved by normalizing to the peak height at mode of distribution; hence, the maximum Y-axis value in the histogram is set at 100%. This approach does not change the shape of the plot, since the only difference is the Y-axis unit, i.e. instead of showing the number of cells, the unit is % versus the total number of cells.

In Fig. 12, the FACS result for A549 cells are present. The results look similar, with anti-CD46 staining giving a markedly shifted peak in comparison with the unstained control and cells stained with isotype antibody. Again, the peaks for anti-CAR and isotype staining gave no result. On the other hand, there was a distinction between the stained cells and unstained control, which was not the case with the HEL cells.

Finally, also 293AD cells were submitted to FACS analysis. Here, better peaks were observed for both CD46 and CAR (Fig. 13). Still, the anti-CAR staining was not sufficient to firmly conclude that 293AD cells do express the CAR receptor. With higher antibody dilutions, the CAR peaks were getting closer. For CD46, the staining was very clear on 293AD cells, giving pronounced individual peaks that were fully separated from the control peaks.

To conclude, higher antibody dilutions can be used than what is indicated by the manufacturers. The procedure for sample preparation and receptor staining was successfully established in HEL, A549 and 293AD cells. The protocol proved useful to detect expression of the CD46 receptor. It is now confident that the cell lines used in this thesis express the CD46 receptor. Compounds interfering with the AdV-CD46 interaction could be possible AdV entry inhibitors. Unfortunately, there was no positive result for CAR staining. Hence, some method modifications (like perhaps testing another anti-CAR antibody or another fluorescent marker than PE) are needed to investigate the expression of CAR on the three cell lines.

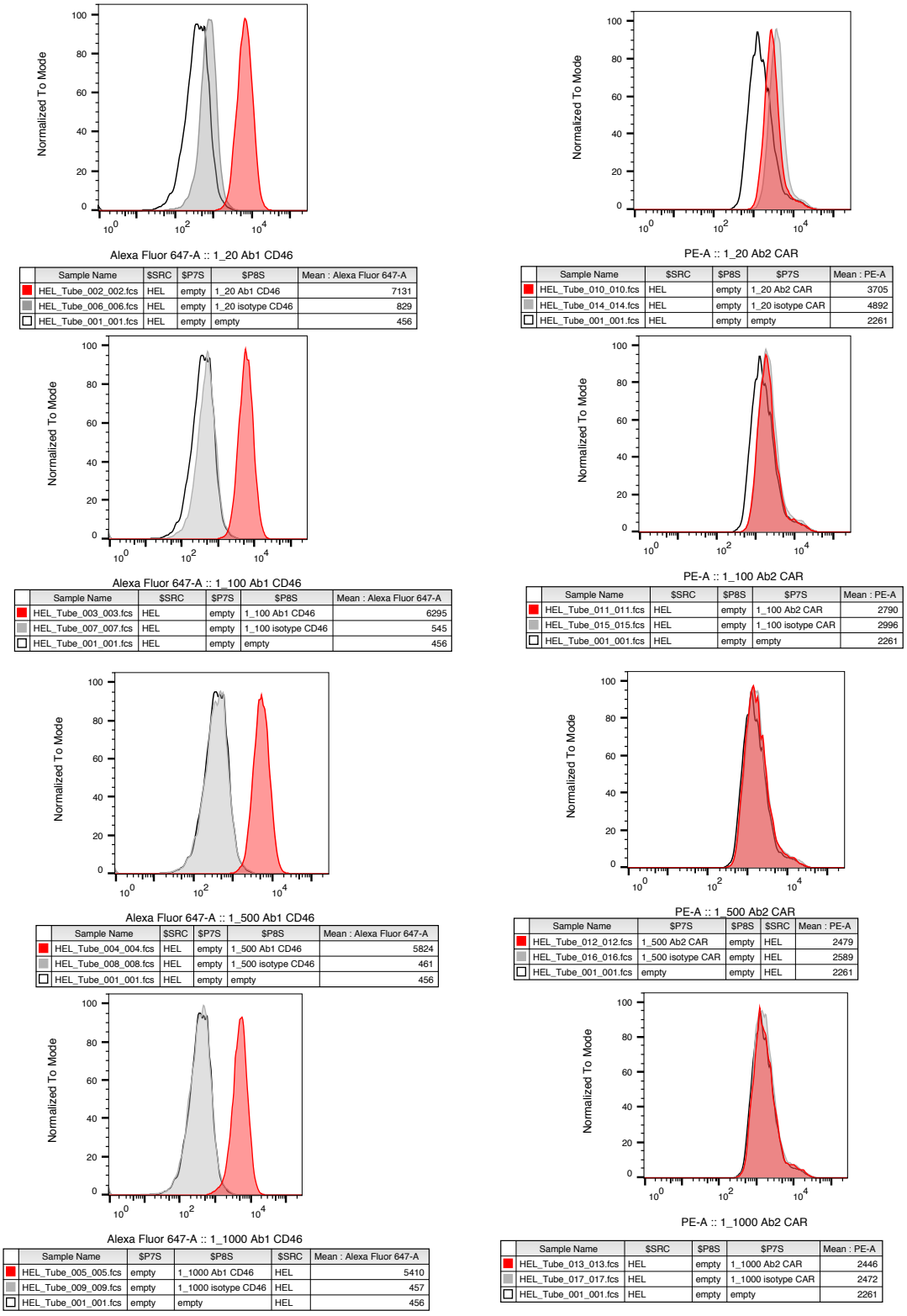

Sample Name	$SRC	$P7S	$P8S	Mean : Alexa Fluor 647-A
HEL_Tube_002_002.fcs	HEL	empty	1_20 Ab1 CD46	7131
HEL_Tube_006_006.fcs	HEL	empty	1_20 isotype CD46	829
HEL_Tube_001_001.fcs	HEL	empty	empty	456

Sample Name	$SRC	$P8S	$P7S	Mean : PE-A
HEL_Tube_010_010.fcs	HEL	empty	1_20 Ab2 CAR	3705
HEL_Tube_014_014.fcs	HEL	empty	1_20 isotype CAR	4892
HEL_Tube_001_001.fcs	HEL	empty	empty	2261

Sample Name	$SRC	$P7S	$P8S	Mean : Alexa Fluor 647-A
HEL_Tube_003_003.fcs	HEL	empty	1_100 Ab1 CD46	6295
HEL_Tube_007_007.fcs	HEL	empty	1_100 isotype CD46	545
HEL_Tube_001_001.fcs	HEL	empty	empty	456

Sample Name	$SRC	$P8S	$P7S	Mean : PE-A
HEL_Tube_011_011.fcs	HEL	empty	1_100 Ab2 CAR	2790
HEL_Tube_015_015.fcs	HEL	empty	1_100 isotype CAR	2996
HEL_Tube_001_001.fcs	HEL	empty	empty	2261

Sample Name	$SRC	$P7S	$P8S	Mean : Alexa Fluor 647-A
HEL_Tube_004_004.fcs	HEL	empty	1_500 Ab1 CD46	5824
HEL_Tube_008_008.fcs	HEL	empty	1_500 isotype CD46	461
HEL_Tube_001_001.fcs	HEL	empty	empty	456

Sample Name	$P7S	$P8S	$SRC	Mean : PE-A
HEL_Tube_012_012.fcs	1_500 Ab2 CAR	empty	HEL	2479
HEL_Tube_016_016.fcs	1_500 isotype CAR	empty	HEL	2589
HEL_Tube_001_001.fcs	empty	empty	HEL	2261

Sample Name	$P7S	$P8S	$SRC	Mean : Alexa Fluor 647-A
HEL_Tube_005_005.fcs	empty	1_1000 Ab1 CD46	HEL	5410
HEL_Tube_009_009.fcs	empty	1_1000 isotype CD46	HEL	457
HEL_Tube_001_001.fcs	empty	empty	HEL	456

Sample Name	$SRC	$P8S	$P7S	Mean : PE-A
HEL_Tube_013_013.fcs	HEL	empty	1_1000 Ab2 CAR	2446
HEL_Tube_017_017.fcs	HEL	empty	1_1000 isotype CAR	2472
HEL_Tube_001_001.fcs	HEL	empty	empty	2261

Figure 11. FACS histograms of HEL cells for detection of CD46 (left panels) and CAR (right panels), analyzed with FlowJo software. The X-axis shows the fluorescent signal while the Y-axis shows the % of cells. The term 'Normalized to Mode' means that a scaling option was applied which normalizes for the area under each curve and scales the Y-axis accordingly. From top to bottom, an antibody dilution of 1/20, 1/100, 1/500 and 1/1000 was used. The peaks represent: in red, anti-CD46 (left) or anti-CAR (right) staining, in grey: isotype control staining, and in black: unstained control. The mean fluorescence signal for these three conditions is shown in the right column of the table below each histogram.

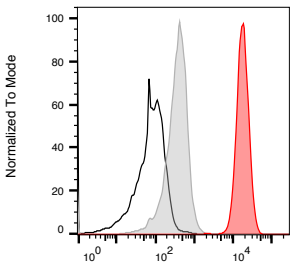

	Sample Name	$SRC	$P7S	$P8S	Mean : Alexa Fluor 647-A
■	A549_Tube_002_019.fcs	A549	empty	1_20 Ab1 CD46	18110
■	A549_Tube_006_023.fcs	A549	empty	1_20 isotype CD46	441
□	A549_Tube_001_018.fcs	A549	empty	empty	89.7

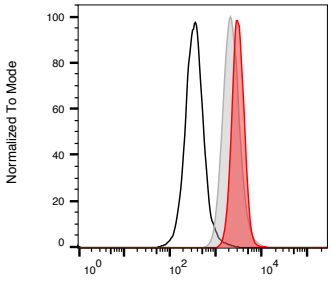

	Sample Name	$SRC	$P8S	$P7S	Mean : PE-A
■	A549_Tube_010_027.fcs	A549	empty	1_20 Ab2 CAR	3261
■	A549_Tube_014_031.fcs	A549	empty	1_20 isotype CAR	2589
□	A549_Tube_001_018.fcs	A549	empty	empty	403

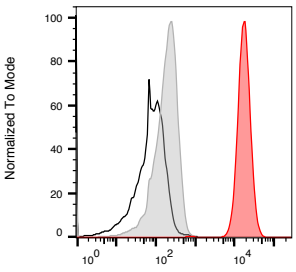

	Sample Name	$SRC	$P7S	$P8S	Mean : Alexa Fluor 647-A
■	A549_Tube_003_020.fcs	A549	empty	1_100 Ab1 CD46	17925
■	A549_Tube_007_024.fcs	A549	empty	1_100 isotype CD46	225
□	A549_Tube_001_018.fcs	A549	empty	empty	89.7

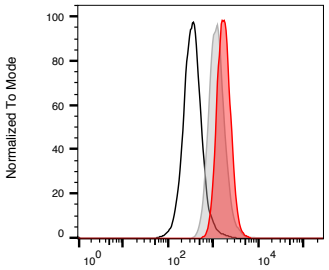

	Sample Name	$SRC	$P8S	$P7S	Mean : Alexa Fluor 647-A
■	A549_Tube_011_028.fcs	A549	empty	1_100 Ab2 CAR	161
■	A549_Tube_015_032.fcs	A549	empty	1_100 isotype CAR	162
□	A549_Tube_001_018.fcs	A549	empty	empty	89.7

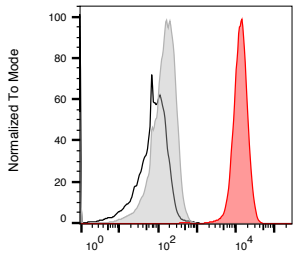

	Sample Name	$SRC	$P7S	$P8S	Mean : Alexa Fluor 647-A
■	A549_Tube_004_021.fcs	A549	empty	1_500 Ab1 CD46	13748
■	A549_Tube_008_025.fcs	A549	empty	1_500 isotype CD46	167
□	A549_Tube_001_018.fcs	A549	empty	empty	89.7

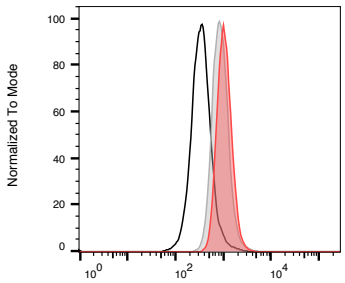

	Sample Name	$SRC	$P8S	$P7S	Mean : PE-A
■	A549_Tube_012_029.fcs	A549	empty	1_500 Ab2 CAR	1160
■	A549_Tube_016_033.fcs	A549	empty	1_500 isotype CAR	964
□	A549_Tube_001_018.fcs	A549	empty	empty	403

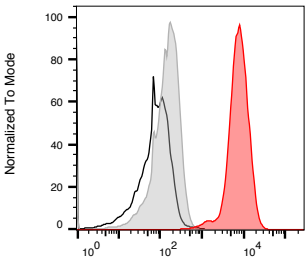

	Sample Name	$SRC	$P7S	$P8S	Mean : Alexa Fluor 647-A
■	A549_Tube_005_022.fcs	A549	empty	1_1000 Ab1 CD46	8313
■	A549_Tube_009_026.fcs	A549	empty	1_1000 isotype CD46	166
□	A549_Tube_001_018.fcs	A549	empty	empty	89.7

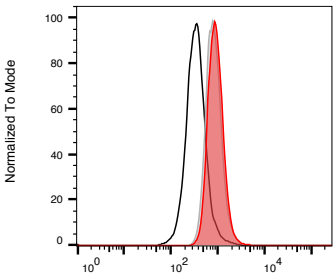

	Sample Name	$SRC	$P8S	$P7S	Mean : PE-A
■	A549_Tube_013_030.fcs	A549	empty	1_1000 Ab2 CAR	987
■	A549_Tube_017_034.fcs	A549	empty	1_1000 isotype CAR	918
□	A549_Tube_001_018.fcs	A549	empty	empty	403

Figure 12. FACS histograms of A549 cells for detection of CD46 (left panels) and CAR (right panels), analyzed with FlowJo software. The X-axis shows the fluorescent signal while the Y-axis shows the % of cells. The term 'Normalized to Mode' means that a scaling option was applied which normalizes for the area under each curve and scales the Y-axis accordingly. From top to bottom, an antibody dilution of 1/20, 1/100, 1/500 and 1/1000 was used. The peaks represent: in red, anti-CD46 (left) or anti-CAR (right) staining, in grey: isotype control staining, and in black: unstained control. The mean fluorescence signal for these three conditions is shown in the right column of the table below each histogram.

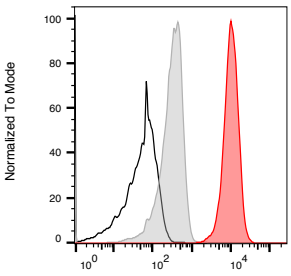

	Sample Name	$SRC	$P7S	$P8S	Mean : Alexa Fluor 647-A
■	hek293_Tube_002_036.fcs	hek293	empty	1_20 Ab1 CD46	10881
■	hek293_Tube_006_040.fcs	hek293	empty	1_20 isotype CD46	357
□	hek293_Tube_001_035.fcs	hek293	empty	empty	54.9

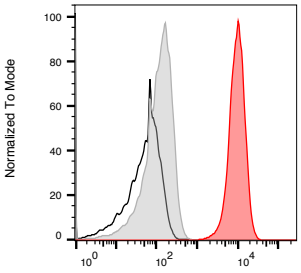

	Sample Name	$SRC	$P7S	$P8S	Mean : Alexa Fluor 647-A
■	hek293_Tube_003_037.fcs	hek293	empty	1_100 Ab1 CD46	10106
■	hek293_Tube_007_041.fcs	hek293	empty	1_100 isotype CD46	129
□	hek293_Tube_001_035.fcs	hek293	empty	empty	54.9

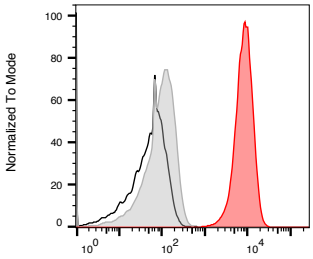

	Sample Name	$SRC	$P7S	$P8S	Mean : Alexa Fluor 647-A
■	hek293_Tube_004_038.fcs	hek293	empty	1_500 Ab1 CD46	8888
■	hek293_Tube_008_042.fcs	hek293	empty	1_500 isotype CD46	105
□	hek293_Tube_001_035.fcs	hek293	empty	empty	54.9

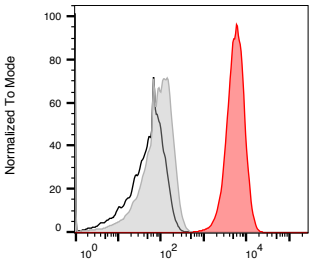

	Sample Name	$SRC	$P7S	$P8S	Mean : Alexa Fluor 647-A
■	hek293_Tube_005_039.fcs	hek293	empty	1_1000 Ab1 CD46	6052
■	hek293_Tube_009_043.fcs	hek293	empty	1_1000 isotype CD46	97.8
□	hek293_Tube_001_035.fcs	hek293	empty	empty	54.9

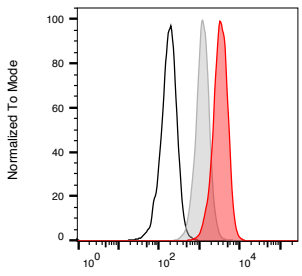

	Sample Name	$SRC	$P8S	$P7S	Mean : PE-A
■	hek293_Tube_010_044.fcs	hek293	empty	1_20 Ab2 CAR	3661
■	hek293_Tube_014_048.fcs	hek293	empty	1_20 isotype CAR	1342
□	hek293_Tube_001_035.fcs	hek293	empty	empty	199

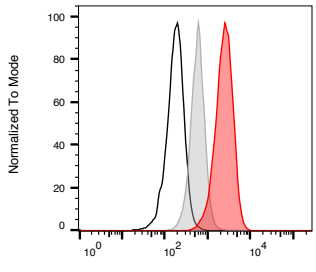

	Sample Name	$SRC	$P8S	$P7S	Mean : PE-A
■	hek293_Tube_011_045.fcs	hek293	empty	1_100 Ab2 CAR	2683
■	hek293_Tube_015_049.fcs	hek293	empty	1_100 isotype CAR	637
□	hek293_Tube_001_035.fcs	hek293	empty	empty	199

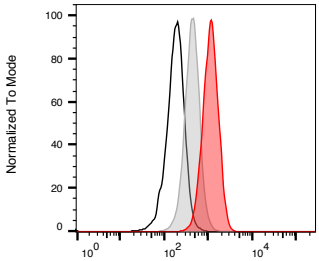

	Sample Name	$SRC	$P8S	$P7S	Mean : PE-A
■	hek293_Tube_012_046.fcs	hek293	empty	1_500 Ab2 CAR	1218
■	hek293_Tube_016_050.fcs	hek293	empty	1_500 isotype CAR	463
□	hek293_Tube_001_035.fcs	hek293	empty	empty	199

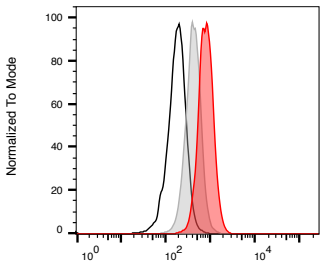

	Sample Name	$SRC	$P8S	$P7S	Mean : PE-A
■	hek293_Tube_013_047.fcs	hek293	empty	1_1000 Ab2 CAR	854
■	hek293_Tube_017_051.fcs	hek293	empty	1_1000 isotype CAR	466
□	hek293_Tube_001_035.fcs	hek293	empty	empty	199

Figure 13. FACS histograms of 293AD cells for detection of CD46 (left panels) and CAR (right panels), analyzed with FlowJo software. The X-axis shows the fluorescent signal while the Y-axis shows the % of cells. The term 'Normalized to Mode' means that a scaling option was applied which normalizes for the area under each curve and scales the Y-axis accordingly. From top to bottom, an antibody dilution of 1/20, 1/100, 1/500 and 1/1000 was used. The peaks represent: in red, anti-CD46 (left) or anti-CAR (right) staining, in grey: isotype control staining, and in black: unstained control. The mean fluorescence signal for these three conditions is shown in the right column of the table below each histogram.

4.3 Anti-AdV evaluation of a broad series of antiviral, cytostatic and immunosuppressive compounds

Among the 30 compounds tested in total (see Table 3 in Materials and Methods), 18 compounds were found to produce some inhibition of AdV replication in HEL cells.

In Table 9, their antiviral EC_{50} values are provided, determined by microscopic scoring of the CPE and by MTS cell viability assay, as well as the cytotoxicity values determined by microscopy (MCC) or MTS assay (CC_{50}). A good correlation between the microscopic and MTS data suggests that the antiviral activity of a test compound is quite robust. Since the reliability of an antiviral test is largely judged by the data obtained with control compounds, the values for the three control compounds will be discussed, i.e. cidofovir, alovudine and zalcitabine, which are nucleoside/nucleotide inhibitors of AdV polymerase. For AdV-2 and AdV-9, their EC_{50} values are quite comparable whether determined by microscopy or MTS assay. This was less evident for AdV-3, AdV-7 and AdV-8. The AdV-8 virus proved to be problematic, since its stock titer was very low (see Table 6) and CPE developed very slowly. For AdV-3 and AdV-7, there is a clear trend towards higher EC_{50} values (for the control compounds) in the MTS compared to CPE assay. Possibly, AdV-3 and AdV-7 may have a less dramatic effect on cell viability, making the MTS assay less reliable for evaluating replication of these two AdV types. With the two virus entry inhibitors $NMSO_3$ and DS-10,000, the EC_{50} values were quite comparable by microscopy and MTS, at least for AdV-2, -3 and -7.

As for the test panel, sirolimus stood out as the most interesting compound with activity across all AdV types and in most cases superior potency (EC_{50} ≤ 0.00128 µM, the lowest concentration tested). Since its EC_{50} values showed large variations, so did the values for its selectivity index (ratio of CC_{50} to EC_{50}) from <1 (AdV-2) to >40,000 (AdV-3, -7 and -9). These determinations should be repeated to achieve final data with less variation. Anyway, this molecule requires further mechanistic investigation (see also section 4.4 and 4.6). Intriguing is the finding that cyclosporin was hardly active, despite the fact that cyclosporin and sirolimus are two immunosuppressive drugs with a complementary (but not overlapping) mechanism of action (see Table 3 in Materials and Methods).

Two other molecules drawing the attention are methotrexate (showing a selectivity index up to 1,666) and mycophenolic acid (showing relatively consistent EC_{50} values). Some AdV inhibition is seen with a range of cytostatic drugs, the most potent one being cladribine (average EC_{50} of 0.12 µM (MTS assay) and 0.41 µM (CPE assay) in AdV-3-infected HEL cells); for gemcitabine, azacytidine, fludarabine, 5-fluorouracil, decitabine and clofarabine, the EC_{50} values were quite high. The antiviral effect of PMEG, an analogue of cidofovir with known anti-DNA virus activity, was as expected.

As for AdV type-dependency, there was a general trend that AdV-2 was less sensitive to the inhibitors than the other AdVs tested. Possibly, a reduction in the multiplicity of infection (by using a more diluted virus) may be needed for AdV-2.

Table 9. Anti-AdV activity and cytotoxicity of the most promising compounds evaluated in HEL cell cultures. The shading indicates strong (dark blue) or moderate (light blue) antiviral activity.

Compound	Concentration unit	Antiviral EC_{50}										Cytotoxicity	
		AdV-2		**AdV-3**		**AdV-7**		**AdV-8**		**AdV-9**		CC_{50}	Minimum cytotoxic concentration
		MTS	visual CPE score	MTS	visual CPE score	MTS	visual CPE score	MTS	visual CPE score	MTS	visual CPE score		
Gemcitabine	µM	>100	>100	69	>100	67	41	>100	>100	2.6	5.3	10	1.3
Azacitidine	µM	>100	>100	65	69	69	70	67	>100	/	>100	>100	>100
Fludarabine	µM	>100	>100	>100	>100	83	48	67	67	>100	76	31	67
Decitabine	µM	>100	82	67	56	80	48	67	79	>100	78	>100	>100
Clofarabine	µM	14	0.47	5.5	0.41	0.031	0.70	0.63	0.080	0.040	0.36	5.3	2.7
Cytarabine	µM	>100	86	>100	>100	78	>100	>100	73	>100	57	75	70
Methotrexate	µM	>100	>100	0.10	0.060	4.8	0.22	0.56	0.45	0.060	0.08	>100	>100
Sirolimus	µM	7.1	4.5	≤0.0013	≤0.00123	≤0.0013	≤0.0013	0.020	≤0.0013	≤0.0013	≤0.0013	53	47
Leflunomide	µM	>100	>100	>100	80	>100	82	66	70	≤0.0013	15	75	>100
DS-10,000	µg/mL	36	16	0.71	1.9	1.5	1.3	83	>100	≤0.0013	4.0	>100	>100
NMSO3	µg/mL	4.0	8.4	0.060	8.9	40	23	>100	82	0.010	38	>100	>100
PMEG	µg/mL	5.3	0.18	5.0	0,20	>10	0.22	>10	>10	>10	>10	>10	>10
Cladribine	µM	3.5	1.9	0.12	0.41	/	1.8	>100	79	0.49	0.32	25	≥20
MPA	µM	10	6.5	5.4	11	5.3	20	1.5	12	0.15	1.4	>100	>100
5-Fu	µM	85	34	54	56	73	20	>100	84	2.7	7.6	>100	>100
Cyclosporine	µM	>10	>10	>10	>10	>10	>10	>10	1.4	>10	>10	51	≥20
Cidofovir	µM	1.4	3.4	0.63	4.3	4.9	5.5	0.010	2.0	1.3	11	>100	>100
Zalcitabine	µM	3.4	5.8	0.090	8.5	0.91	9.8	18	3.1	1.2	4.9	>100	>100
Alovudine	µM	3.1	1.9	0.020	2.8	<0.0032	3.7	<0.0032	6.6	1.1	1.2	>100	>100

Table 10. Anti-AdV activity and cytotoxicity of the most promising compounds evaluated in A549 cell cultures. The shading indicates strong (dark blue) or moderate (light blue) antiviral activity.

Compound	Concentration unit	Antiviral EC_{50}										Cytotoxicity	
		AdV-2		**AdV-3**		**AdV-7**		**AdV-8**		**AdV-9**		CC_{50}	Minimum cytotoxic concentration
		MTS	visual CPE score	MTS	visual CPE score	MTS	visual CPE score	MTS	visual CPE score	MTS	visual CPE score		
Gemcitabine	µM	>100	>100	>100	>100	>100	>100	>100	>100	>100	>100	1.0	0.42
Azacitidine	µM	>100	>100	>100	>100	>100	>100	>100	>100	64	>100	84	≥4.0
Fludarabine	µM	>100	>100	>100	>100	>100	>100	>100	>100	>100	>100	0.19	0.10
Decitabine	µM	98	>100	>100	>100	>100	>100	>100	>100	>100	>100	20	≥4.0
Clofarabine	µM	>100	>100	>100	>100	>100	>100	>100	>100	>100	>100	0.48	0.28
Cytarabine	µM	>100	>100	>100	>100	>100	>100	>100	>100	>100	>100	1.0	0.42
Methotrexate	µM	>100	>100	>100	>100	>100	>100	>100	>100	>100	>100	0.080	0.32
Sirolimus	µM	>100	>100	>100	>100	>100	>100	>100	>100	92	>100	71	50
Leflunomide	µM	>100	>100	>100	>100	>100	>100	>100	>100	>100	>100	>100	>100
DS-10,000	µg/mL	74	>100	>100	>100	>100	>100	>100	>100	>100	>100	>100	>100
NMSO3	µg/mL	29	34	45	>100	>100	>100	21	12	6.5	52	>100	>100
PMEG	µg/mL	0.84	1.2	>100	>100	>100	>100	>100	>100	>10	0.059	17	3.7
Cladribine	µM	>100	>100	>100	>100	>100	>100	>100	>100	>100	>100	10	12
MPA	µM	>100	>100	>100	>100	>100	>100	>100	>100	>100	>100	2.0	2.4
5-Fu	µM	>100	>100	>100	>100	>100	>100	>100	>100	>100	>100	5.6	2.2
Cyclosporine	µM	>100	>100	>100	>100	82	>100	>100	>100	>100	>100	4.3	≥0.0013
Cidofovir	µM	26	40	14	35	18	22	>100	50	>100	57	95	80
Zalcitabine	µM	0.63	1.2	1.1	3.2	1.0	0.78	1.2	2.2	6.9	0.76	>100	>100
Alovudine	µM	0.010	0.10	0.020	0.090	0.080	0.15	<0.0032	0.010	0.040	0.18	99	>100

Compared to the data in HEL cells, the compounds showed, in general, much less pronounced anti-AdV activity in A549 cells (Table 10). Here, the control compound cidofovir as well as the two entry inhibitors $NMSO_3$ and DS-10,000, were much less active. Two other controls, zalcitabine and alovudine, were strongly active. Neither of the immunosuppressant or cytostatic agents gave moderate anti-AdV inhibition in A549 cells, which is possibly related to the fact that all these molecules had pronounced cytotoxicity in faster growing A549 cells compared to resting HEL cells. The inactivity of sirolimus in A549 cells contrasted sharply with its remarkable effect in HEL cells, and suggests some differences in the AdV replication strategy in these two cell lines, which warrants further mechanistic investigation.

Table 11. Overview of the inactive compounds evaluated in HEL cell cultures.

Compound	Concentration unit	Antiviral EC_{50}										Cytotoxicity	
		AdV-2		**AdV-3**		**AdV-7**		**AdV-8**		**AdeV-9**		CC_{50}	Minimum cytotoxic concentration
		MTS	visual CPE score	MTS	visual CPE score	MTS	visual CPE score	MTS	visual CPE score	MTS	visual CPE score		
HHA	µg/mL	>100	>100	>100	>100	>100	>100	/	/	>100	>100	3.3	≥20
UDA	µg/mL	>100	>100	>100	>100	>100	>100	>100	>100	>100	>100	78	47
GNA	µg/mL	>100	>100	>100	>100	80	73	>100	>100	>100	>100	>100	73
WGA	µg/mL	>100	>100	>100	>100	>100	>100	>100	>100	>100	>100	9.6	11
Imatinib	µM	>100	>100	>100	>100	>100	>100	>100	>100	>100	>100	26	>100
PRM-S	µg/mL	>100	>100	>100	>100	>100	>100	>100	>100	>100	>100	>100	>100
Tacrolimus	µM	>100	>100	>100	>100	>100	>100	>100	>100	>100	>100	52	>100
Imiquimod	µM	>100	>100	>100	>100	>100	>100	>100	>100	>100	>100	>100	>100
TFT	µM	>100	>100	>100	>100	>100	>100	>100	>100	>100	>100	>100	>100
PFA	µM	>100	>100	>100	>100	/	/	>100	>100	>100	>100	>100	>100
Ara-A	µM	>100	>100	92	60	>100	>100	>100	>100	>100	>100	>100	>100
Ribavirin	µM	87	100	70	84	>100	>100	>100	>100	87	79	>100	>100

Finally, an overview is given of the inactive molecules in Table 11 (HEL cells) and Table 12 (A549 cells). Despite the fact that ribavirin has been evaluated in some case studies in AdV-infected individuals [1], its direct effect on AdV replication is hardly visible. There was no inhibition with carbohydrate-binding agents, i.e. four lectin compounds (HHA, UDA, GNA and WGA) and the antibiotic pradimicin, and a few cytostatic/immunomodulatory agents. Furthermore, Table 12 shows that some compounds were slightly active in A549 cells, but not in HEL cells (Table 11). Specifically, imatinib showed antiviral activity in AdV-3- and AdV-9-infected A549 cells, while this compound was not active in HEL cells regardless of which AdV type was tested.

Table 12. Overview of the inactive compounds evaluated in A549 cell cultures. The light blue shading indicates moderate antiviral activity.

Compound	Concentration unit	Antiviral EC_{50}[c]										Cytotoxicity	
		Adenovirus-2		**Adenovirus-3**		**Adenovirus-7**		**Adenovirus-8**		**Adenovirus-9**		CC_{50}[a]	Minimum cytotoxic concentration[b]
		MTS	visual CPE score	MTS	visual CPE score	MTS	visual CPE score	MTS	visual CPE score	MTS	visual CPE score		
HHA	µg/mL	>100	>100	>100	>100	>100	>100	/	/	28	>100	>100	≥4.0
UDA	µg/mL	>100	>100	>100	>100	>100	>100	>100	>100	>100	>100	19	2.2
GNA	µg/mL	>100	>100	>100	>100	>100	>100	>100	>100	25	>100	>100	>100
WGA	µg/mL	>100	>100	>100	>100	>100	>100	>100	>100	>100	>100	23	12
Imatinib	µM	12	15	>100	>100	0.20	>100	>100	>100	0.40	3.2	0.40	3.2
PRM-S	µg/mL	>100	>100	>100	>100	>100	>100	13,7	>100	>100	>100	>100	60
Tacrolimus	µM	>100	>100	>100	>100	>100	>100	>100	>100	>100	>100	28	20
Imiquimod	µM	>100	>100	76	73	75	86	>100	>100	>100	>100	>100	>100
TFT	µM	>100	>100	>100	>100	>100	>100	2.6	>100	>100	>100	51	0.80
PFA	µM	>100	>100	53	60	67	>100	>100	>100	>100	>100	>100	>100
Ara-A	µM	>100	>100	>100	>100	>100	>100	>100	>100	>100	>100	89	20
Ribavirin	µM	85	>100	>100	>100	>100	>100	>100	>100	>100	>100	>100	60

4.4 Preliminary result for the effect of sirolimus on AdV replication assessed by virus yield assay

Intrigued by the strong effect of sirolimus on AdV replication in HEL cells, some more mechanistic experiments were performed to understand this effect.
First, a qPCR-based method was used to verify whether sirolimus reduces the virus yield (i.e. the number of AdV particles released in the supernatant). Three compounds, i.e. cidofovir, alovudine and zalcitabine were included as controls. The method was established by Naesens *et al.* some time ago [6]. The availability of a qPCR plasmid standard (see Materials and Methods) allowed to convert the C_T-values into the number of AdV DNA copies. Based on these numbers, the log_{10}-reduction in copy number was calculated for each compound concentration. Using GraphPad software, the data were plotted into a dose response curve shown in Fig. 14. Here, a reduction of 1 log_{10} or 2 log_{10} indicates that the AdV copy number was reduced by 10- or 100-fold, respectively.

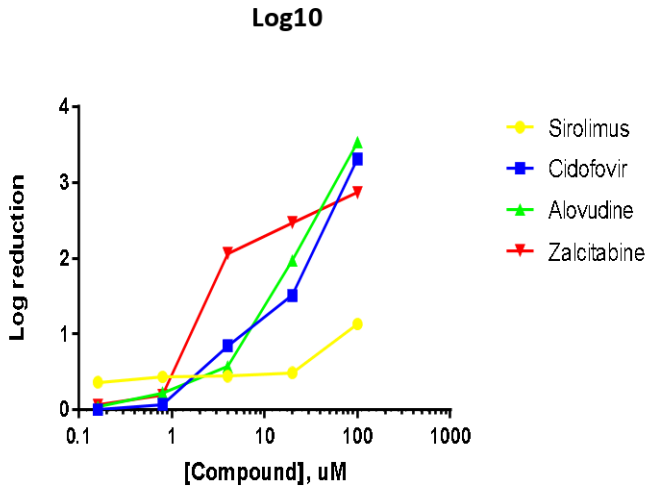

Figure 14. Dose-dependent reduction in AdV yield in AdV-infected HEL cells treated with sirolimus or the reference compounds cidofovir, alovudine and zalcitabine. The Y-axis shows the log_{10}-reduction in AdV copy number, based on qPCR analysis of the supernatants.

Whereas the three reference compounds produced a nice dose-dependent effect reaching more than 3 log_{10} (i.e. 1000-fold) reduction (Fig. 14), the anti-AdV-2 effect was surprisingly low for sirolimus. Even at 100 µM, the highest concentration tested, sirolimus gave only 1 log_{10} (i.e. a 10-fold) reduction in the number of AdV particles released in the supernatant. This result is very different from the convincing anti-AdV effect seen with sirolimus in the CPE reduction assay in HEL cells (Table 12). Still, the effect of sirolimus in the CPE assay was lower for AdV-2 compared to the other AdV types, potentially explaining the rather disappointing result in the qPCR assay. Hence, the qPCR-based virus yield assay needs to be repeated on the HEL supernatants collected for the other AdV-types, which will hopefully give better results for inhibition of sirolimus on the AdV DNA level.

4.5 Development of fluorescence microscopical assay with the AdV-5-GFP vector

When AVP011 is added to HEL or A549 cells, replication-incompetent AdV-5 are produced, giving a prominent GFP signal but no CPE or formation of virus particles. This is related to the fact that the AdV-5-GFP vector AVP011 is deleted in the AdV E1 and E3 regions; since the E1 proteins (essential for the assembly of virus particles) are not formed, the AdV life cycle is interrupted. Viral replication can occur only in cell lines, such as 293A cell, that provide the E1 region.

Therefore, the GFP reporter signals visible in Fig. 15 and Fig. 16 do not represent multicycle virus replication, but only the replication steps preceding late gene expression, including virus entry. By investigating whether a given test compound does or does not reduce the GFP signal in AVP011-infected HEL or A549 cells, it may conclude whether this compound acts before or after late gene expression. For instance, the method would be very interesting to study AdV entry inhibitors. In relationship to the antiviral data in this project, it would be interesting to verify that DS-10,000 and PMEG are indeed only active in infected HEL cells, whereas imatinib is only active in A549 cells. This could not only confirm that the anti-AdV activity of these molecules is cell line-dependent, since also a first insight into their mechanism (i.e. acting before or after AdV late gene expression) could be provided.

Due to the time limit, it was unable to do these AVP011 experiments with test compounds. However the time-lapse fluorescence assay on live cells was optimized, in which the GFP signal is followed after adding the AVP011 vector to HEL or A549 cells. In Figs. 15 and 16, two snapshots taken on day 0 and 2 p.i. are shown. Overall, the % green cells is quite comparable for HEL and A59 cells, indicating a similar infection ratio.

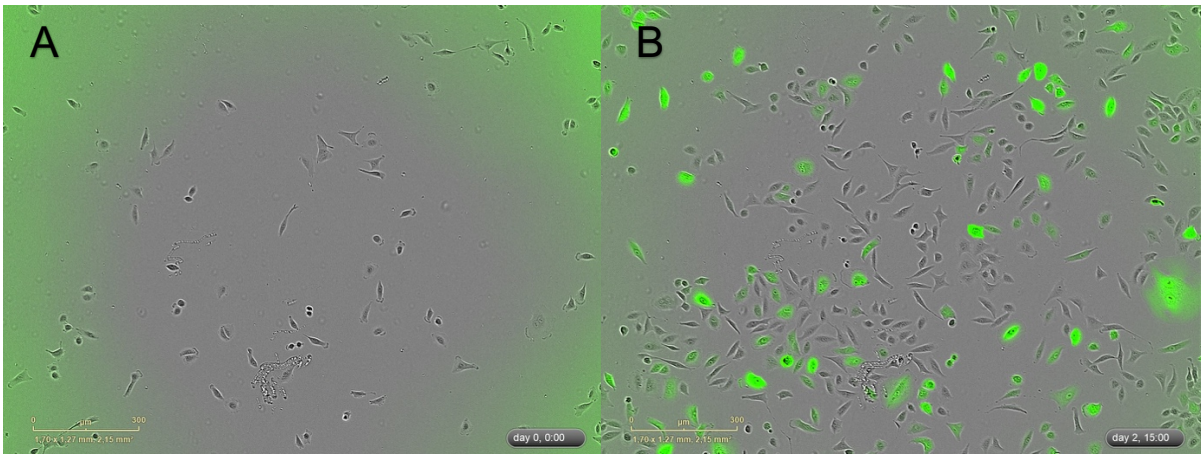

Figure 15. GFP signal in A549 cells infected with the AdV5-GFP (AVP011) vector. Time-lapse fluorescence microscopy was performed; the photographs show the cells at day 0 (A) and day 2 (B) post infection.

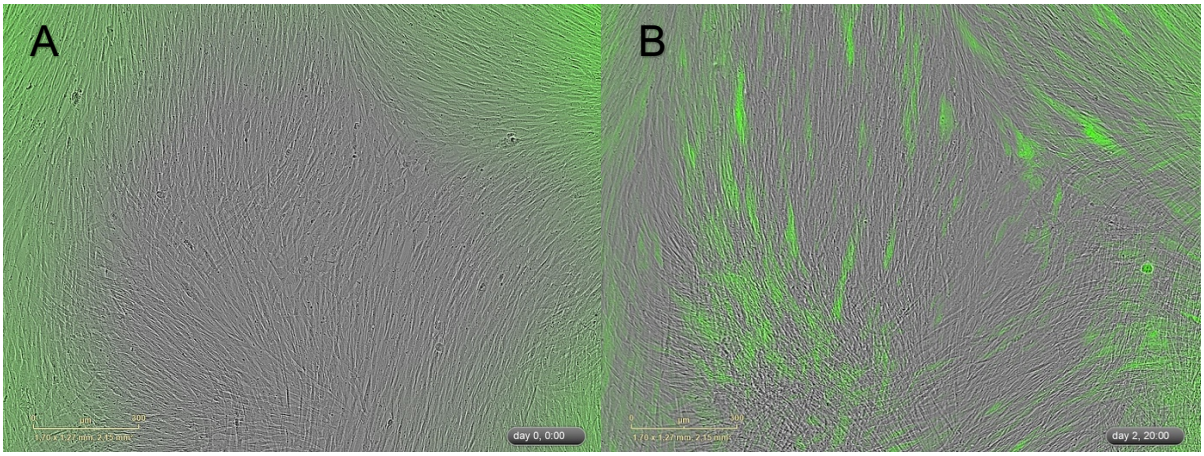

Figure 16. GFP signal in HEL cells infected with the AdV5-GFP (AVP011) vector. Time-lapse fluorescence microscopy was performed; the photographs show the cells at day 0 (A) and day 2 (B) post infection.

4.6 Application of the ELISA assay for measuring mTOR activation

Although the ELISA kit to measure mTOR activation is very user-friendly, its usefulness markedly depends on whether the results with a positive control are sufficiently robust. During this project, a few conditions were compared to achieve a useful positive control.

The results from one pilot experiment are shown in Table 16, with in the right column the OD values minus background (i.e. OD value for the well receiving incubation buffer). As expected, serum-starved cells gave a lower signal than control cells receiving FCS all the way. Of the four mTOR activator conditions that were tested, three were not working, i.e. 20% FCS, 2 mM glutamine and 50 nM Calyculin A for 15 min. The only mTOR activating treatment found to be effective (i.e. giving a signal higher than that of serum-starved cells) was 50 nM Calyculin A for 30 min, hence this can be used in future experiments.

Unfortunately, the dynamic range of this ELISA assay was not as expected, since the difference between the control- and serum-starved cells was only 0.3154 OD, which is lower than the background signal (incubation buffer). This means that all experiments will have to be executed on duplo or even triplo wells to acquire reliable data. If performed in this manner, this easy ELISA assay can be useful to assess mTOR activation in AdV-infected HEL cells and the inhibitory effect of sirolimus.

Table 13. First results of the mTOR ELISA assay.

Cell treatment condition	$OD_{450\ nm}$ value	$OD_{450\ nm}$ value minus background
Incubation buffer	0.3651	0.0000
Control cells receiving serum	1.1218	0.7567
Starved cells (i.e. no serum for 48 h)	0.8064	0.4413
Starved cells + 1 h 20% FCS	0.6287	0.2636
Starved cells + 1 h 2 mM glutamine	0.6832	0.3181
Starved cells + 15' 50 nM Calyculin A	0.7125	0.3474
Starved cells + 30' 50 nM Calyculin A	1.0997	0.7346

5. Conclusion

At the start of this project, the AdV virus stocks were available, however virus titration and verification of AdV identity was still required. For virus quantification, the end-point dilution virus titration method was successfully used. Within the laboratory, a robust and easy sequencing protocol was implemented to verify the identity of AdV stocks, that is based on sequencing of a short AdV hexon fragment using a pair of universal primers. This sequencing protocol optimized in this master thesis will be routinely used during future AdV work.

The same is true for the FACS analysis of AdV receptor expression. The methods for cell detachment and antibody staining were optimized, and are now ready to use for detection of the CD46 receptor, which proved to be present on the three cell lines that were used in this project. Since 293AD cells showed very clear CD46 peaks, this cell line is an ideal positive control. The assay will have high value to investigate entry inhibitors interfering with the AdV-CD46 interaction. For detection of CAR, new antibodies will have to be purchased. Availability of a good control cell line (e.g. cells transfected with a CAR expression plasmid) would also be helpful.

In the broad antiviral evaluation, most anti-AdV activity was seen in HEL cells, whereas only a few compounds proved effective in A549 cells. This is a pity since A549 cells are more practical given that they grow much faster than HEL cells. Also, HEL cells can only be passaged for about 15 passages, while A549 are a continuous cell line.

In general, less antiviral activity in AdV-2-infected HEL cells was observed compared to the other AdV types, indicating that perhaps a more diluted AdV-2 is needed to slightly reduce the multiplicity of infection. The result was different in A549 cells, in which more compounds were active against AdV-2 and AdV-9 compared to the other AdV types. This illustrates that AdV replication as well as the mechanism of action of an AdV inhibitor, can be markedly cell-line dependent. This was particularly clear for sirolimus, since this molecule gave nice anti-AdV effect in HEL cells, but not in A549 cells.

The findings provide a basis to further investigate the anti-AdV activity of a number of immunosuppressive/cytostatic molecules, the most interesting one being sirolimus. To understand the different impact of sirolimus on AdV replication in the two cell lines, more research is needed. Therefore, an ELISA assay for mTOR pathway activity was implemented, the target of sirolimus. Within the time frame of this thesis, it was only possible to demonstrate mTOR activation with a positive control, hence the ELISA method is now ready to conduct experiments with AdV and sirolimus. Similarly, the fluorescence microscopy-based method that was established with the AdV5-GFP vector, is ready for testing the inhibitors that are picked up in the antiviral CPE reduction assay in HEL or A549 cells.

To conclude, diverse AdV protocols were successfully developed using a variety of techniques, like (fluorescence) microscopy, cell viability testing, qPCR, FACS and ELISA. In the very near future, these methods will be particularly useful to confirm the anti-AdV activity of the hit compounds, and reveal their basic anti-AdV mechanism of action.

References

[1] L. Lenaerts, E. De Clercq, and L. Naesens, "Clinical features and treatment of adenovirus infections," vol. 18, ed, 2008, pp. 357-374.

[2] C. A. Lindemans, A. M. Leen, and J. J. Boelens, "How I treat adenovirus in hematopoietic stem cell transplant recipients," *Blood,* vol. 116, no. 25, pp. 5476-5485, 2010, doi: 10.1182/blood-2010-04-259291.

[3] L. Lenaerts, "Mouse adenovirus as a model for adenovirus pathogenesis and tropism," Leuven : K.U.Leuven. Faculteit Geneeskunde, 2008.

[4] M. Strand, "The discovery of antiviral compounds targeting adenovirus and herpes simplex virus: assessment of synthetic compounds and natural products," ed, 2014.

[5] H. L. H. Liapis and H. L. W. H. L. Wang, *Pathology of Solid Organ Transplantation edited by Helen Liapis, Hanlin L. Wang*. Berlin, Heidelberg : Springer Berlin Heidelberg, 2011.

[6] L. Naesens *et al.*, "Antiadenovirus Activities of Several Classes of Nucleoside and Nucleotide Analogues," *Antimicrobial Agents and Chemotherapy,* vol. 49, no. 3, p. 1010, 2005.

[7] Y.-C. Lee *et al.*, "Human adenovirus type 8 epidemic keratoconjunctivitis with large corneal epithelial full-layer detachment: an endemic outbreak with uncommon manifestations.(CASE SERIES)(Report)," vol. 9, p. 953, 2015, doi: 10.2147/OPTH.S79697.

[8] R. C. Hoeben and T. G. Uil, "Adenovirus DNA replication," *Cold Spring Harbor perspectives in biology,* vol. 5, no. 3, p. a013003, 2013, doi: 10.1101/cshperspect.a013003.

[9] A. Dhingra *et al.*, "Molecular Evolution of Human Adenovirus (HAdV) Species C," *Scientific Reports,* vol. 9, no. 1, p. <xocs:firstpage xmlns:xocs=""/>, 2019, doi: 10.1038/s41598-018-37249-4.

[10] L. Coughlan *et al.*, "Tropism-Modification Strategies for Targeted Gene Delivery Using Adenoviral Vectors," *Viruses,* vol. 2, no. 10, pp. 2290-2355, 2010, doi: 10.3390/v2102290.

[11] Y. P. Dewi. "Replication of DNA Virus Genomes." SlideShare. https://www.slideshare.net/yrprmtdw/replication-of-dna-virus-genomes (accessed May 21, 2016.

[12] S. J. Flint, V. R. Racaniello, G. F. Rall, A. M. Skalka, and L. W. Enquist, *Principles of virology*, 4th ed. ed. Washington, DC : ASM Press, 2015.

[13] N. Arnberg, "Adenovirus receptors: implications for targeting of viral vectors," *Trends in Pharmacological Sciences,* vol. 33, no. 8, pp. 442-448, 2012, doi: 10.1016/j.tips.2012.04.005.

[14] C. Patzke *et al.*, "The coxsackievirus-adenovirus receptor reveals complex homophilic and heterophilic interactions on neural cells," *The Journal of neuroscience : the official journal of the Society for Neuroscience,* vol. 30, no. 8, pp. 2897-2910, 2010, doi: 10.1523/JNEUROSCI.5725-09.2010.

[15] B. D. Persson *et al.*, "Structure of the Extracellular Portion of CD46 Provides Insights into Its Interactions with Complement Proteins and Pathogens (Structure of CD46 Ectodomain)," *PLoS Pathogens,* vol. 6, no. 9, p. e1001122, 2010, doi: 10.1371/journal.ppat.1001122.

[16] J. M. Chamberlain *et al.*, "Cidofovir Diphosphate Inhibits Adenovirus 5 DNA Polymerase via both Nonobligate Chain Termination and Direct Inhibition, and Polymerase Mutations Confer Cidofovir Resistance on Intact Virus," *Antimicrobial agents and chemotherapy,* vol. 63, no. 1, 2019, doi: 10.1128/AAC.01925-18.

[17] S. Matthes-Martin *et al.*, "European guidelines for diagnosis and treatment of adenovirus infection in leukemia and stem cell transplantation: summary of ECIL -4 (2011," vol. 14, ed, 2012, pp. 555-563.

[18] F. M. Marty *et al.*, "A Randomized, Double-Blind, Placebo-Controlled Phase 3 Trial of Oral Brincidofovir for Cytomegalovirus Prophylaxis in Allogeneic Hematopoietic Cell Transplantation," *Biology of Blood and Marrow Transplantation,* vol. 25, no. 2, pp. 369-381, 2019, doi: 10.1016/j.bbmt.2018.09.038.

[19] D. F. Florescu *et al.*, "Safety and Efficacy of CMX001 as Salvage Therapy for Severe Adenovirus Infections in Immunocompromised Patients," *Biology of Blood and Marrow Transplantation,* vol. 18, no. 5, pp. 731-738, 2012, doi: 10.1016/j.bbmt.2011.09.007.

[20] D. I. Chigbu and B. A. Labib, "Pathogenesis and management of adenoviral keratoconjunctivitis," *Infection and Drug Resistance,* vol. 11, pp. 981-993, 2018.
[21] R. Caraballo *et al.*, "Triazole linker-based trivalent sialic acid inhibitors of adenovirus type 37 infection of human corneal epithelial cells," *Org. Biomol. Chem.,* vol. 13, no. 35, pp. 9194-9205, 2015, doi: 10.1039/c5ob01025j.
[22] J. Hillenkamp *et al.*, "Topical treatment of acute adenoviral keratoconjunctivitis with 0.2% cidofovir and 1% cyclosporine: a controlled clinical pilot study. (Clinical Sciences)," *Archives of Ophthalmology,* vol. 119, no. 10, p. 1487, 2001, doi: 10.1001/archopht.119.10.1487.
[23] A. Mac Sweeney *et al.*, "Discovery and structure-based optimization of adenain inhibitors," *ACS medicinal chemistry letters,* vol. 5, no. 8, pp. 937-941, 2014, doi: 10.1021/ml500224t.
[24] G. Wadell and N. Arnberg. "Innovative solution for treatment of viral eye infection." Adenovir Pharma AB. https://www.adenovir.com/about-the-project/ (accessed 21 may 2019.
[25] M. Bleakley and S. R. Riddell, "Molecules and mechanisms of the graft-versus-leukaemia effect," vol. 4, M. Bleakley, Ed., ed, 2004, pp. 371-380.
[26] M. Samaniego, B. N. Becker, and A. Djamali, "Drug Insight: maintenance immunosuppression in kidney transplant recipients," *Nature Clinical Practice Nephrology,* vol. 2, no. 12, pp. 688-699, 2006, doi: 10.1038/ncpneph0343.
[27] V. Le Sage, A. Cinti, R. Amorim, and A. J. Mouland, "Adapting the Stress Response: Viral Subversion of the mTOR Signaling Pathway," *Viruses,* vol. 8, no. 6, 2016, doi: 10.3390/v8060152.
[28] M. A. Ramakrishnan, "Determination of 50% endpoint titer using a simple formula," *World journal of virology,* vol. 5, no. 2, pp. 85-86, 2016, doi: 10.5501/wjv.v5.i2.85.
[29] P. Fanourgiakis *et al.*, "Intravesical Instillation of Cidofovir in the Treatment of Hemorrhagic Cystitis Caused by Adenovirus Type 11 in a Bone Marrow Transplant Recipient," *Clinical Infectious Diseases,* vol. 40, no. 1, pp. 199-201, 2005, doi: 10.1086/426594.
[30] M. H. Beers, R. S. Porter, T. V. Jones, J. L. Kaplan, and M. Berkwits, *The Merck Manual of diagnosis and therapy*, eighteenth edition ed. Whitehouse Station : Merck Research Laboratories, 2006.
[31] N. Dey, P. De, and B. Leyland-Jones, *PI3K-mTOR in Cancer and Cancer Therapy edited by Nandini Dey, Pradip De, Brian Leyland-Jones*. Cham : Springer International Publishing : Imprint Humana Press, 2016.
[32] S. C. Yates *et al.*, "Dysfunction of the mTOR pathway is a risk factor for Alzheimer's disease.(Report)," *Acta Neuropathologica Communications,* vol. 1, no. 1, 2013, doi: 10.1186/2051-5960-1-3.